

FINAL REPORT

Thermal Destruction of PFAS by Hydrodynamic Cavitation

Michael Izenson
Rachel Gilmore
Creare LLC

Gabrielle David
*US Army Engineering Research and Development Center, Cold Regions Research and
Engineering Laboratory*

Anthony Bednar
ERDC-Environmental Laboratory

January 2023

REPORT DOCUMENTATION PAGE					Form Approved OMB No. 0704-0188	
<p>The public reporting burden for this collection of information is estimated to average 1 hour per response, including the time for reviewing instructions, searching existing data sources, gathering and maintaining the data needed, and completing and reviewing the collection of information. Send comments regarding this burden estimate or any other aspect of this collection of information, including suggestions for reducing the burden, to Department of Defense, Washington Headquarters Services, Directorate for Information Operations and Reports (0704-0188), 1215 Jefferson Davis Highway, Suite 1204, Arlington, VA 22202-4302. Respondents should be aware that notwithstanding any other provision of law, no person shall be subject to any penalty for failing to comply with a collection of information if it does not display a currently valid OMB control number.</p> <p>PLEASE DO NOT RETURN YOUR FORM TO THE ABOVE ADDRESS.</p>						
1. REPORT DATE (DD-MM-YYYY) 27-01-2023		2. REPORT TYPE SERDP Final Report			3. DATES COVERED (From - To) 12/6/2021 - 12/6/2022	
4. TITLE AND SUBTITLE Thermal Destruction of PFAS by Hydrodynamic Cavitation					5a. CONTRACT NUMBER 22-P-0004	
					5b. GRANT NUMBER	
					5c. PROGRAM ELEMENT NUMBER	
6. AUTHOR(S) Michael Izenson and Rachel Gilmore: Creare LLC Gabrielle David: US Army Engineering Research and Development Center, Cold Regions Research and Engineering Laboratory Anthony Bednar: ERDC-Environmental Laboratory					5d. PROJECT NUMBER ER21-1018	
					5e. TASK NUMBER	
					5f. WORK UNIT NUMBER	
7. PERFORMING ORGANIZATION NAME(S) AND ADDRESS(ES) Creare LLC 16 Great Hollow Road Hanover, NH 03755					8. PERFORMING ORGANIZATION REPORT NUMBER TM-4970C	
9. SPONSORING/MONITORING AGENCY NAME(S) AND ADDRESS(ES) Strategic Environmental Research and Development Program (SERDP) 4800 Mark Center Drive, Suite 16F16 Alexandria, VA 22350-3605					10. SPONSOR/MONITOR'S ACRONYM(S) SERDP	
					11. SPONSOR/MONITOR'S REPORT NUMBER(S) ER21-1018	
12. DISTRIBUTION/AVAILABILITY STATEMENT DISTRIBUTION STATEMENT A. Approved for public release: distribution unlimited.						
13. SUPPLEMENTARY NOTES						
14. ABSTRACT Per- and polyfluoroalkyl substance (PFAS) contamination of groundwater is pernicious and widespread, potentially contaminating the drinking water of millions of Americans. A major source of this contamination is aqueous film forming foam which was used for decades for firefighting and is still in use today . The Department of Defense has identified hundreds of military sites where water has been contaminated by PFAS and a full DoD clean-up effort is expected to cost billions of dollars. Existing options to destroy PFAS are limited and expensive. We have demonstrated a novel technique for thermal destruction of PFAS. The low-cost process uses hydrodynamic cavitation (HC) to thermally destroy PFAS in water. We optimized flow parameters using methylene blue dye to measure oxidation rates across a wide range of conditions. We then demonstrated destruction of perfluorooctanesulfonic acid (PFOS) by HC in a series of tests that show the effects of reactor design and operating conditions. We measured the rates of PFOS destruction as well as concentration of reaction products as a function of time after starting the process. We found that HC was a robust process that effectively destroyed PFAS across the range of conditions tested.						
15. SUBJECT TERMS Thermal Destruction, PFAS, Hydrodynamic Cavitation, environmental restoration, treatment of PFAS-impacted matrices, thermal treatment, PFAS thermal treatment						
16. SECURITY CLASSIFICATION OF:			17. LIMITATION OF ABSTRACT UNCLASS	18. NUMBER OF PAGES 74	19a. NAME OF RESPONSIBLE PERSON Michael Izenson	
a. REPORT UNCLASS	b. ABSTRACT UNCLASS	c. THIS PAGE UNCLASS			19b. TELEPHONE NUMBER (Include area code) 603-640-3800	

This report was prepared under contract to the Department of Defense Strategic Environmental Research and Development Program (SERDP). The publication of this report does not indicate endorsement by the Department of Defense, nor should the contents be construed as reflecting the official policy or position of the Department of Defense. Reference herein to any specific commercial product, process, or service by trade name, trademark, manufacturer, or otherwise, does not necessarily constitute or imply its endorsement, recommendation, or favoring by the Department of Defense.

TABLE OF CONTENTS

1	ABSTRACT.....	1
1.1	OBJECTIVES	1
1.2	TECHNICAL APPROACH.....	1
1.3	RESULTS	1
1.4	BENEFITS	2
2	OBJECTIVE	2
3	BACKGROUND	3
3.1	THE NEED	3
3.2	SONOLYTIC PFAS DESTRUCTION	4
3.3	HC REACTORS	5
3.3.1	Methylene Blue as a Proxy Indicator of Hydroxyl Radical Generation	7
4	MATERIALS AND METHODS.....	7
4.1	HC REACTOR.....	7
4.2	METHYLENE BLUE ANALYSIS METHODS	9
4.3	PFAS ANALYSIS METHODS	10
4.4	DATA REDUCTION	10
5	RESULTS AND DISCUSSION.....	11
5.1	EVALUATE CAVITATION INTENSITY.....	11
5.2	EVALUATE REACTOR DESIGN AND OPERATING CONDITIONS FOR HYDROXYL RADICAL GENERATION	12
5.3	EVALUATE PFAS DESTRUCTION	14
5.4	BYPRODUCTS OF PFAS DESTRUCTION	16
5.5	ANALYZE SCALABILITY	19
6	CONCLUSIONS AND IMPLICATIONS FOR FUTURE RESEARCH /IMPLEMENTATION.....	21
7	LITERATURE CITED	23
8	APPENDICES	28

LIST OF FIGURES

Figure 1.	Proposed Process for Thermal Destruction of PFAS by Hydrodynamic Cavitation (HC)	2
Figure 2.	Bubble Radius and Temperature and Pressure Inside a Bubble During Collapse.	4
Figure 3.	Bench-Scale HC Test Facility for PFOS Testing	8
Figure 4.	HC Reactor Test Loop in a Fume Hood at Creare During Testing With PFOS and After Updates to Reduce the Pressure Drop in The System Loop.	8
Figure 5.	Spectrometer Installed on and Held Above Sight Glass in Reactor Test Loop.....	9
Figure 6.	Spectrometer Calibration.....	10
Figure 7.	Experimental Conditions Tested With Distilled Water.....	11
Figure 8.	Photos of Cavitation in the $\gamma = 0.14$, Seven Orifice Plate and the $\gamma = 0.25$, Single Orifice Plate.....	12

Figure 9.	Absorbance Spectra, Concentration Decay Curve, and Photographs of the Orifice Plate at Select Times in an Experiment with Methylene Blue and the $\gamma = 0.14$ Single Orifice.	12
Figure 10.	Experimental Results From Testing With PFOS.....	14
Figure 11.	Experimental Results From 24-Hour Test With PFOS	15
Figure 12.	Photos of Orifice Plate at Conclusion of Testing With PFOS.....	16
Figure 13.	Byproducts of PFOS Degradation After 240 Minutes in the HC Reactor	17
Figure 14.	Byproducts of PFOS Degradation at the End of a 4-Hour and a 24-Hour Experiment in the HC Reactor	17

LIST OF TABLES

Table 1.	Test Conditions With Methylene Blue (MB)	13
Table 2.	Average Operating Conditions During PFOS Experiments.....	16
Table 3.	Fluorine Measured After HC Reactor Experiment Conclusion	18
Table 4.	Measured PFOS Concentrations from Samples Taken During Experiment Setup ...	18
Table 5.	Potential PFAS Treatment Scenarios	21
Table 6.	Calibration Data Collected During PFAS Analysis	28
Table 7.	Shorter-Chain PFAS Byproduct.....	29

LIST OF ACROYNYS

DoD	Department of Defense
GAC	granular-activated carbon
HC	hydrodynamic cavitation
H ₂ O ₂	hydrogen peroxide
LHA	lifetime health advisory
PFAS	per- and polyfluoroalkyl substances
PFOA	perfluorooctanoic acid
PFOS	perfluorooctanesulfonic acid

KEY WORDS

PFAS, environmental remediation

1 ABSTRACT

1.1 OBJECTIVES

The objective is to develop a simple, low-cost method to destroy per- and polyfluoroalkyl substances (PFAS). PFAS destruction is a critical technology for environmental remediation because PFAS contamination of groundwater is pernicious and widespread, potentially contaminating the drinking water of up to 110 million Americans (EWG 2019). A major source of this contamination is aqueous film forming foam, which was used for decades for firefighting and is still in use today (ITRC 2018). The Department of Defense (DoD) has identified at least 425 military sites where water has been contaminated by PFAS, and a full DoD cleanup effort is expected to surpass \$2B (Beitsch 2019). Currently, options to destroy PFAS are limited and expensive. The dominant method for removing aqueous PFAS is sorption using granular-activated carbon (GAC) or ion-exchange resins (ITRC 2018). This method results in contaminated GAC or resin which must be incinerated at high temperature ($> 1100^{\circ}\text{C}$) to destroy the PFAS (ITRC 2018). This incineration step is energy-intensive and may produce undesirable byproducts, necessitating improved technologies for PFAS destruction. We proposed hydrodynamic cavitation (HC) as a novel and potentially less expensive alternative technology for thermal destruction of PFAS in water, and we conducted research to investigate its feasibility and scalability.

1.2 TECHNICAL APPROACH

PFAS substances are exceptionally stable, so destroying them requires extreme reaction conditions. We hypothesized that HC could generate the high temperatures and oxidation conditions needed to destroy PFAS substances in a process that is scalable and does not produce toxic byproducts. Our research builds on prior literature that demonstrated PFAS destruction by ultrasonic cavitation (Moriwaki et al. 2005). Researchers have shown how the high temperatures and pressures produced by collapsing cavitation bubbles enable complete breakdown of PFAS into nontoxic byproducts via pyrolytic removal of the ionic head group, pyrolytic breakage of the carbon chain, and oxidative breakage of the C-F bonds (Vecitis et al. 2009). We hypothesized that the same mechanisms for PFAS destruction occur in cavitation produced by HC. We believe this hypothesis is sound because the prior literature shows that HC is a viable method for destruction of other persistent water contaminants such as chloroform and dyes (Braetigam et al. 2010; Gogate and Bhosale 2013). In this limited-scope project, we conducted an experimental study to investigate the effects of HC reactor parameters on PFAS destruction. We performed lab testing of the byproducts produced, and analyzed how the experimental results from our lab-scale testing would scale up to use in the field.

1.3 RESULTS

We have shown that HC can degrade perfluorooctanesulfonic acid (PFOS) across a wide range of operating conditions. Single-pass destruction efficiencies are currently up to 0.03%, and we hope to improve this efficiency by at least one or two orders of magnitude with further research and development. Results of these tests indicate that it may be feasible to use HC to destroy PFAS chemicals on a scale that is relevant to the DoD and commercial water treatment facilities. Lessons learned from these exploratory tests can be applied to improve future experiments.

1.4 BENEFITS

We have demonstrated that HC is a feasible technology for thermal destruction of PFAS and have deepened our understanding of the important reactor parameters. In the near term, a successful program will foster expanded R&D, allowing further experimental and computational study of the reaction conditions produced by HC and the resulting PFAS destruction pathways and kinetics. Further R&D would also allow exploration into other factors needed for successful scale-up of the technology. Long-term results of a successful program will be the deployment of HC facilities that support cost-effective and efficient DoD and municipal remediation of PFAS-contaminated sites.

2 OBJECTIVE

This research responds to the call for development of new thermal destruction technologies that improve the cost effectiveness and sustainability of processes for treating PFAS-laden materials. We propose a novel thermal destruction technology based on HC (Figure 1). Cavitation bubble collapse is a proven effective method for PFAS destruction; however, prior work uses ultrasonic cavitation to produce the bubbles, and ultrasound is difficult to apply in large-scale treatment systems. We hypothesize that (1) PFAS will be destroyed as effectively by HC cavitation as by ultrasonic cavitation; and (2) HC treatment has the potential to be more cost effective and sustainable than existing technologies for treatment of PFAS-laden water streams, such as contaminated drinking water or the residual product streams from nano-filtration, reverse osmosis, or regeneration of ion-exchange resins. We hypothesize that HC can generate the high temperatures and oxidation conditions needed to destroy PFAS substances in a process that is scalable and does not produce toxic byproducts.

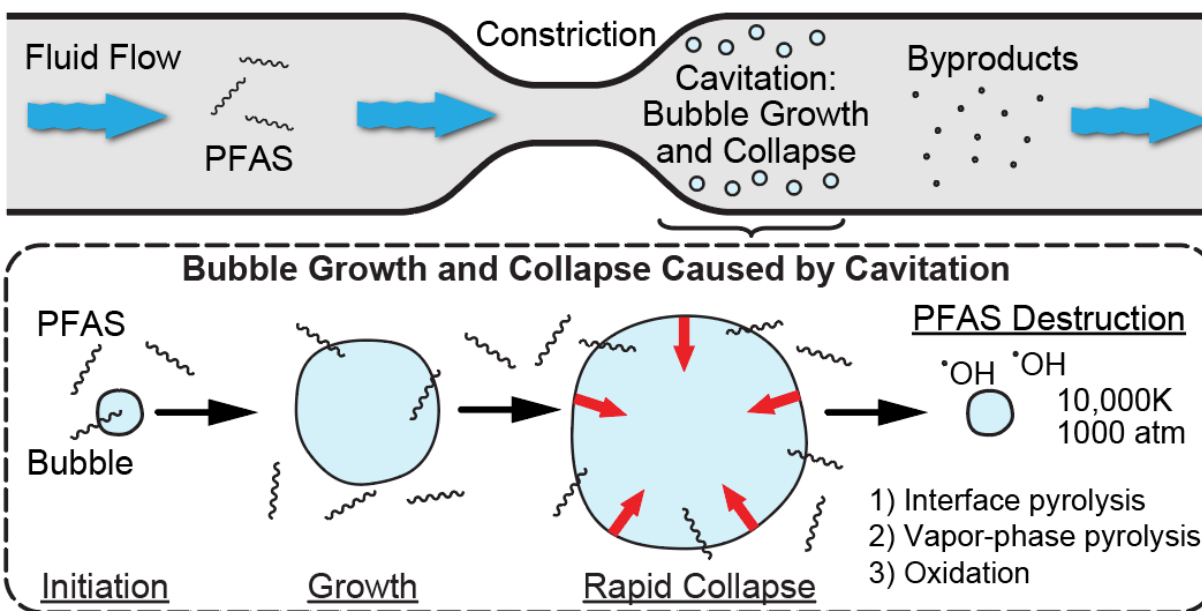


Figure 1. Proposed Process for Thermal Destruction of PFAS by Hydrodynamic Cavitation (HC)

The goals of this limited-scope project were to answer the following technical questions:

1. What reactor design and operating parameters are needed for a lab-scale HC facility to produce the intense localized pressure, temperature, and oxidation conditions needed to destroy PFAS, and how do these design and operating parameters affect the rate of PFAS destruction?
2. What, if any, toxic byproducts are produced by lab-scale HC destruction of PFAS, and how are these byproducts affected by reactor design and operating parameters?
3. Is it feasible to use HC technology to destroy PFAS at large scale in the field?

A successful project will demonstrate that HC is a feasible technology for thermal destruction of PFAS and will further inform our understanding of the important reactor and process parameters. In the near term, a successful program will lead to additional R&D, allowing further experimental and computational study of the reaction conditions produced by HC and the resulting PFAS destruction pathways and kinetics. Further R&D would also allow exploration into other factors needed for successful scale-up of the technology. Long-term results of a successful program will be the deployment of HC facilities that support cost-effective and efficient remediation of PFAS-contaminated sites.

3 BACKGROUND

A growing number of communities are finding their groundwater contaminated with PFAS substances. Improved understanding of PFAS destruction mechanisms and their suitability for use in large-scale treatment systems are needed to meet the increasing demand for PFAS treatment technology.

3.1 THE NEED

PFAS substances are highly resistant to breakdown in the environment and pose risks to developmental, immune, metabolic, and endocrine health throughout the U.S. (Hu et al. 2016). Unfortunately, PFAS contamination of groundwater is widespread with the drinking water of up to 110 million Americans potentially contaminated (EWG 2019). The DoD identified 564 public or private drinking water systems that tested above the EPA LHA (lifetime health advisory) level of 70 ppt as of August 2017 (Sullivan 2018). This number is increasing as additional water sources are tested and currently includes at least 425 military sites nationwide (Beitsch 2019). The Washington, DC-based nonprofit Environmental Working Group and the Social Science Environmental Health Research Institute at Northeastern University maintain an interactive map of affected sites (EWG 2019). As of July 2019, they had identified known PFAS contamination in 712 locations in 49 states. Some of these sites had PFAS concentrations over 100,000 ppt (EWG 2019).

In July 2018, our home state of New Hampshire adopted regulatory limits of 12 ppt for perfluorooctanoic acid (PFOA), 15 ppt for PFOS, 18 ppt for perfluorohexanesulfonic acid, and 11 ppt for perfluorononanoic acid (Ropeik 2019). These standards require local water systems to begin sampling for PFAS on a quarterly basis starting in October 2019. If average PFAS levels over the first year of testing exceed the regulatory limits, municipalities must begin planning for how to remove it from their water. The State of New Hampshire estimates this process could cost

up to \$190 million over the next two years. This cost for a single state is dwarfed by the estimate that, if mandated, a full nationwide DoD cleanup would surpass \$2B (Beitsch 2019).

While the dominant method to remove aqueous PFAS is sorption using GAC or ion-exchange resins (ITRC 2018), this method results in contaminated GAC or resin which must be incinerated at high temperature ($> 1100^{\circ}\text{C}$) to destroy the PFAS (ITRC 2018). This incineration step is energy intensive and may produce undesirable byproducts. Novel PFAS water treatment processes with lower installation and operating costs than traditional GAC and ion-exchange resin approaches to capture and incinerate PFAS could have substantial appeal and market share, and could reduce the financial burden on the DoD and municipalities to comply with environmental regulations.

3.2 SONOLYTIC PFAS DESTRUCTION

It is well known that cavitation and bubble collapse can generate extremely high local temperature conditions, comparable to those traditionally achieved in an incinerator (Figure 2). Several researchers have reported success using ultrasound-generated cavitation (also called sonolysis) for PFAS destruction in laboratory-scale studies (Moriwaki et al. 2005; Vecitis et al. 2008; Campbell et al. 2009; Campbell and Hoffman 2015; Rodriguez-Freire et al. 2015; Fernandez et al. 2016; and Gole et al. 2018). For example, Moriwaki et al. (2005) showed that collapsing bubbles produced conditions that were extreme enough to break C-F bonds in PFOS, producing fluoride and sulfate as the primary degradation products.

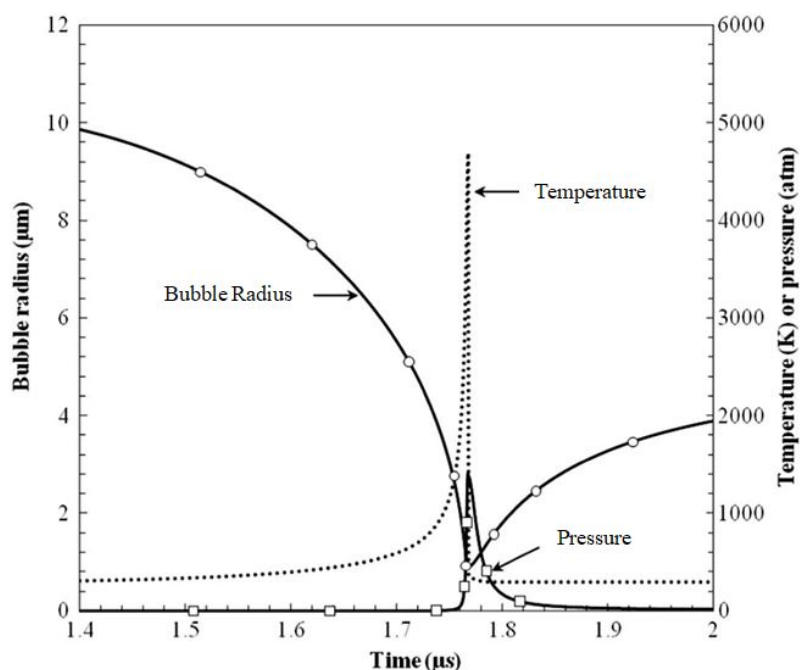


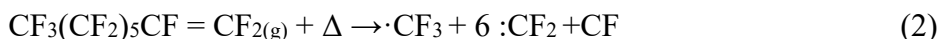
Figure 2. Bubble Radius and Temperature and Pressure Inside a Bubble During Collapse (Merouani et al. 2014). Temperatures in collapsing bubbles can reach up to 10,000 K.

Vecitis et al. (2008, 2009) have presented a proposed decomposition pathway for aqueous perfluorooctane substances such as PFOS and PFOA via sonolysis. For PFOS, the pathway is as follows:

1. Pyrolysis at the bubble interface cleaves the C–S bond:



2. Pyrolysis in the bubble vapor breaks fluorocarbon intermediates into C1 fluororadical constituents:



3. C1 fluororadicals react with H_2O , HO , H , and O-atom in the bubble vapor to yield CO , CO_2 , and HF byproducts. HO , H , and O-atom are generated by thermolytic splitting of water in the bubble vapor.

Other studies on sonochemical degradation of PFOS under different experimental conditions (sound frequency, initial PFOS concentration, reactor setup) disagree with this mechanism and find that defluorination can occur at higher rates than the cleavage of the sulfonic head (Rodriguez-Freire et al. 2015). It is important to note that ultrasonic cavitation appears to fully break down PFAS under at least some experimental conditions (Vecitis et al. 2008), removing the ionic head-group, breaking the carbon chain, and breaking the C-F bonds. Complete breakdown of PFAS chemicals is desirable because short chain fluorocarbons may also be hazardous and are more difficult to remove with conventional technologies. Thus allowing fluororadicals to remain is considered producing toxic byproducts that may require additional treatment steps.

3.3 HC REACTORS

Ultrasonic cavitation is difficult to apply for large-scale water treatment. An alternative process to generate and violently collapse bubbles is by HC. In HC, a region of low static pressure is created by accelerating water through a Venturi nozzle or orifice plate. As the water velocity increases, the static pressure falls. If the local static pressure falls below the water's vapor pressure, then bubbles form and grow in the water. When the water decelerates and static pressure recovers, the bubbles rapidly collapse. Extremely high local pressure and temperature conditions arise when the liquid decelerates abruptly at the end of the rapid collapse.

The maximum temperatures and pressures and the rate of hydroxyl radical production from HC bubble collapse have been well studied using experimental and computational methods (Moholkar and Pandit 1997; Moholkar et al. 1999; Kanthale et al. 2005; Krishnan et al. 2006; Sharma et al. 2008; Zhang et al. 2008; Kumar et al. 2012; Capocelli et al. 2014a; Capocelli et al. 2014b; Soyama and Hoshino 2016; Pawar et al. 2017; Li et al. 2017; Wu et al. 2018; Bandala and Rodriguez-Narvaez 2019; and Cappa et al. 2020). Experimental methods include high-speed video, acoustic monitoring of cavitation intensity and the use of model reactions (such as methylene blue dye) to monitor hydroxyl radical production. Computational methods include using software, such as Fluent, to conduct single- and two-phase simulations.

HC and hybrid reactors employing HC have been demonstrated for the destruction of a wide range of organic and nonorganic compounds including chloroform and dyes (Cheng et al.

2008; Braeutigam 2010; Gogate and Bhosale 2013; Capocelli et al. 2014; Tao et al. 2016; Pawar et al. 2017; Suryawanshi et al. 2018; Gagol et al. 2018; Thanekar and Gogate 2018; Bandala and Rodriguez-Narvaez 2019; and Burzio 2019). Hybrid reactors predominantly use oxidizing reagents to supplement the thermolytic production of hydroxyl radicals in the collapsing bubbles.

Several reactor parameters and operating conditions have been identified that predict the intensity of HC bubble formation and collapse. These include the method and geometry that produce the rapid static pressure drop and recovery, the cavitation number, and the recovery pressure.

Constriction Geometry. In the currently proposed project, we plan to induce the rapid static pressure drop and recovery using an orifice plate. We choose to use an orifice plate due to its simplicity and low cost of prototyping. Orifice geometry is characterized by the dimensionless number γ , which is the ratio of the total flow area of the orifice to the cross-sectional area of the pipe. In the case where the orifice plate contains multiple orifices:

$$\gamma = \frac{Nd^2}{D^2} \quad (3)$$

where D is the pipe diameter, d is the diameter of an orifice, and N is the number of orifices in the plate. For an orifice plate with a single orifice in the center of the plate, γ simplifies to d^2/D^2 , which is the square of the familiar dimensionless number $\beta = d/D$ that is used to characterize orifice flow meters. γ values of 0.1 to 0.2 typically give good performance in the HC systems cited. The geometry of the orifice, such as the plate thickness (or the convergence and divergence angles in the case of a Venturi nozzle), is also an important factor, affecting the size of the cavitation cloud and the energy released by each individual bubble collapse. Pawar et al. (2017) found that orifices produce smaller clouds than Venturi nozzles, but those clouds had more intense bubble collapse.

Cavitation Number. Whether or not cavitation will occur is predicted by the dimensionless number, C_V , which is defined as:

$$C_V = \frac{P_2 - P_{sat}(T)}{0.5\rho(v_2/C_c)^2 - \Delta P_{exp,I}} \quad (4)$$

where P_2 is the recovery pressure, P_{sat} is the temperature-dependent vapor pressure of the liquid, ρ is the density of the liquid, v_2 is the velocity at the throat of the constriction, C_c is given by:

$$C_c = 1 - \frac{1-\gamma}{2.08(1-\gamma)+0.5371} \quad (5)$$

and $\Delta P_{exp,I}$ is given by:

$$\Delta P_{exp,I} = (1 - \gamma)^2 0.5\rho v_2^2. \quad (6)$$

Cavitation occurs when the cavitation number is equal to or less than one. Lower cavitation numbers generally indicate more intense cavitation, although research indicates that an optimal value of C_v exists for a given reactor (Soyama and Hoshino 2016). Typical values of C_v used in treatment of contaminants in water range from 0.1 to 1.

Recovery Pressure. The researchers cited found that recovery pressures greater than one atmosphere (~0.25 to 0.5 MPa) are needed to yield violent bubble collapse and hydroxyl radical production. In addition, the level and frequency of turbulence downstream of the cavitation initiation site determines if bubble collapse is transient, resulting in high peak pressures and temperatures, or oscillating, resulting in less extreme peak conditions (Moholkar and Pandit 1997; Kanthale et al. 2005). This result indicates that the conditions downstream of the constriction must be controlled and monitored closely.

Based on our review of the literature, we expect that by properly specifying the HC reactor design and operating parameters, the same extreme reaction conditions that destroy PFAS by acoustic cavitation can be achieved with HC. The previous success of HC reactors to treat other contaminants further supports our hypothesis that HC can be used to destroy PFAS.

3.3.1 Methylene Blue as a Proxy Indicator of Hydroxyl Radical Generation

Hydroxyl radicals are important to breaking the C-F bonds in PFAS and achieving complete degradation, rather than simply generating shorter-chain fluorocarbons, which may be even more challenging to remove than their longer-chain counterparts. Since measuring the PFAS concentration is time consuming, we used methylene blue as a proxy chemical that could help us probe the reactor design and operating conditions best suited to generating these hydroxyl radicals. Methylene blue is a hydroxyl radical scavenger that changes color from blue to clear when reduced and has been used as an indicator for $\bullet\text{OH}$ generation in HC (Li et al. 2017). We can use a straightforward absorbance measurement to monitor the methylene blue concentration in real time. Methylene blue is a non-volatile polar molecule, so it will exist primarily in the liquid phase rather than in the vapor bubbles formed during HC (Li et al. 2017). Therefore, it is destroyed through reaction with hydroxyl radicals, rather than through pyrolysis in the collapsing bubbles. Methylene blue reacts with $\bullet\text{OH}$ in a 1:1 molar ratio. To degrade PFAS chemicals, we expect to need a 1:1 molar ratio of fluorine atoms and $\bullet\text{OH}$, plus additional $\bullet\text{OH}$ to account for that consumed in reactions with any co-contaminants in the water to be remediated. We will use methylene blue to narrow down the set of operating conditions at which we will test with PFAS.

4 MATERIALS AND METHODS

4.1 HC REACTOR

As part of a previous project funded by the EPA SBIR program, we built a lab-scale HC facility at Creare for treating PFAS. The test facility uses an orifice plate to generate cavitation conditions. Under that project, we operated the lab-scale facility under a small set of conditions and demonstrated a detectable level of PFAS destruction. We reconstructed and modified the test facility for use on this project and measured performance over a larger range of operating conditions.

Figure 3 shows a schematic, and Figure 4 shows a photo of the test facility setup. The system uses 0.375" ID 316 stainless steel tube in the main test loop (highlighted in blue). A LiquiFlo Model H9 316 stainless steel gear pump drives the flow. We took care to avoid materials containing fluorocarbons in the gears, bearings and wear plates, and seals. For this project, we replaced the flow meter used in prior testing, as the previous flow meter had been unstable. We also built an in-line spectrometer to get real-time measurements of the methylene blue concentration as described further in Section 4.2.

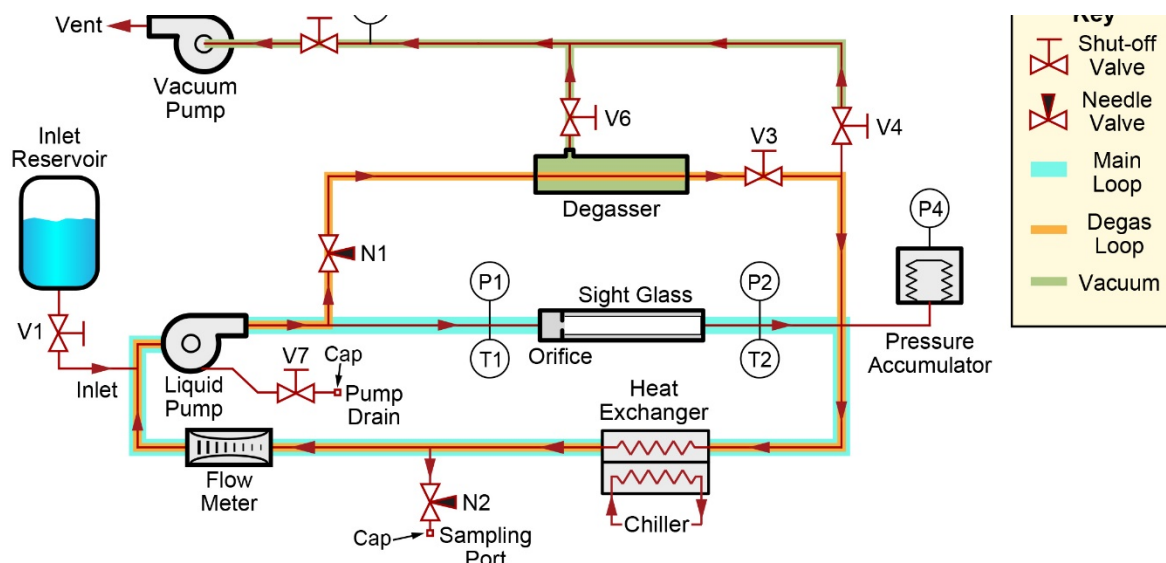


Figure 3. Bench-Scale HC Test Facility for PFOS Testing

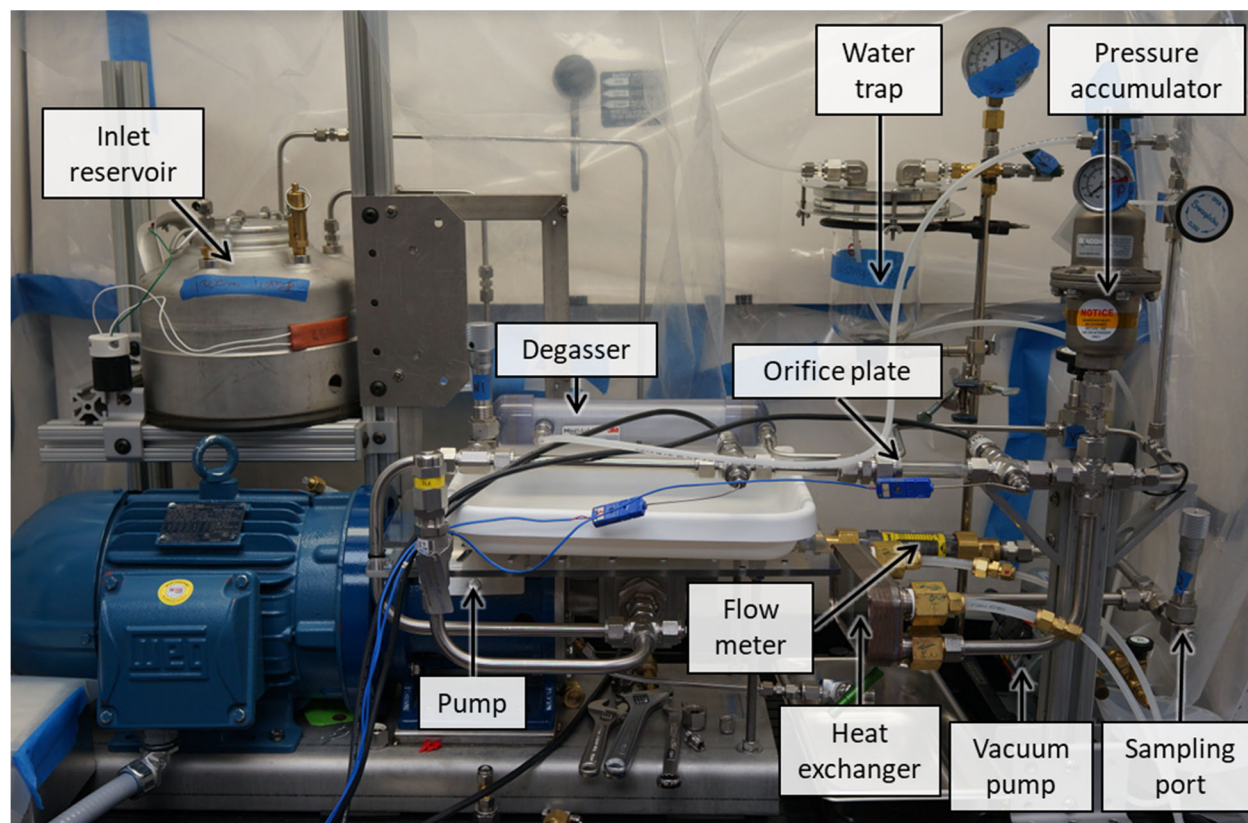


Figure 4. HC Reactor Test Loop in a Fume Hood at Creare During Testing With PFOS and After Updates to Reduce the Pressure Drop in The System Loop.

We found that at high pump speeds and flow rates, the Carbon 60 wear plates and bearings in the pump were producing a black powder debris that contaminated the process fluid and complicated optical absorption measurements. We discussed this with the pump manufacturer, and they suggested trying PEEK wear plates. Unfortunately, these also showed excessive wear and

generated small flakes that clogged the orifice plates. Upon further investigation of other material options, we also discovered that the PEEK material also contains a small amount of PTFE, making it further unsuitable for testing with PFAS. We therefore disassembled our system and thoroughly cleaned it to remove any traces of fluorocarbon materials and debris from the pump. We then returned to using Carbon 60 bearings and wear plates. Overall, we found that the current pump is not well suited to higher flow rate testing in our system loop. We identified an alternate pump that is better suited, but it had a long lead time of 20 weeks that was not feasible within the project timeline. For the remainder of this project, we avoided operating the system at the high pump speeds and flow rates that caused problems previously, while knowing that this limited the maximum destruction efficiency we were able to achieve.

4.2 METHYLENE BLUE ANALYSIS METHODS

We designed and built a spectrometer to measure the light absorption properties of the circulating methylene blue solution through a sight glass in our test loop (Figure 5). Before each experiment, we collect a background signal with the spectrometer LED off but the spectrometer installed on the sight glass and a reference signal with the spectrometer installed on an identical sight glass filled with water. The spectra are sufficiently stable that we do not need to repeat these measurements for a given experiment.

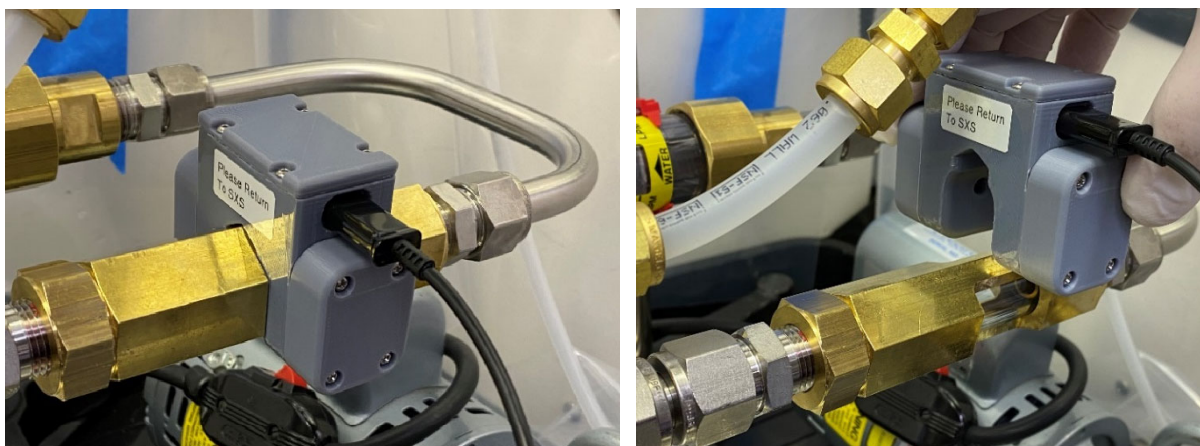


Figure 5. Spectrometer Installed on (left) and Held Above (right) Sight Glass in Reactor Test Loop

We calibrated the in-line spectrometer using methylene blue solutions of known concentrations. The steps for interpreting the data are shown in Figure 6. First, we calculate the absorbance from the measured transmittance, reference, and background signals:

$$A = -\log_{10} \left(\frac{\text{signal} - \text{background}}{\text{reference} - \text{background}} \right) \quad (7)$$

and plot these spectra in the left panel of Figure 6. Second, we calculate the average absorbance between 3.2 and 3.34 eV for each spectrum and subtract this value from the spectrum at that time point. This is not critical for these reference samples but is important for some of the experiments when the pump bearing and wear plate debris causes scattering that appears as a uniform offset of the absorbance spectra. Third, we integrate each corrected absorbance spectra between 2.0 and 2.18 eV. From the normalized calibration spectra shown in the middle panel of Figure 6, we can see that the shape of the spectra is independent of the concentration in this region and integrating

reduces error in the calibration from random noise in the measured spectra. Finally, we use the calibration shown in the right panel of Figure 6 to determine the methylene blue concentration from the integrated absorbance intensity. We note that this calibration is not linear, as would be expected by Beer's law because the sight glass is cylindrical, so the light is passing through a curved surface rather than the typical flat cuvette wall, and this distorts the absorbance spectrum. Since we have developed this calibration specifically for this geometry, we are confident it gives accurate concentration results for our experiments; it would not be relevant for measurements made in a typical spectrometer with a cuvette. We considered trying to get or make a sight glass with flat windows, but determined that the challenges associated with doing so as well as the potential dead zones in the flow and increased pressure drop associated with changing the tubing shape and diameter would outweigh the benefits of a more straightforward absorption measurement.

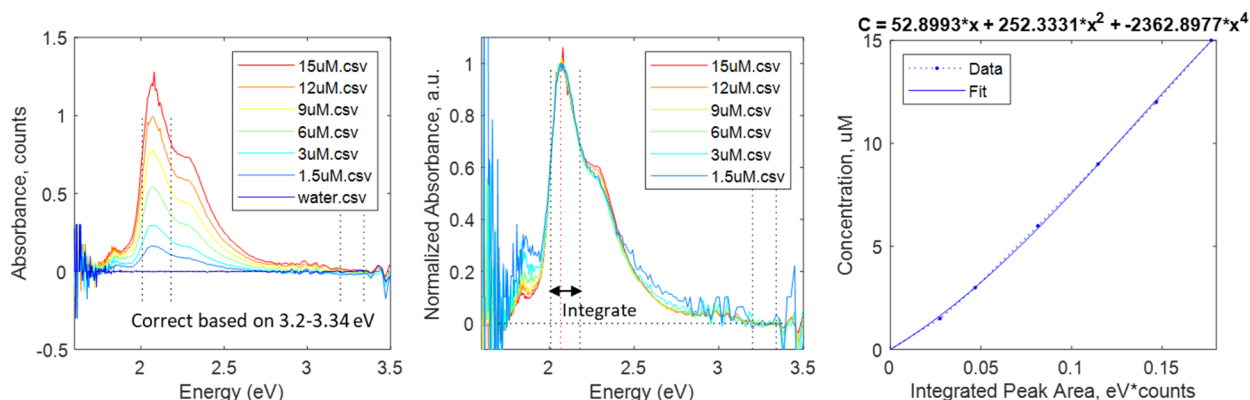


Figure 6. Spectrometer Calibration

4.3 PFAS ANALYSIS METHODS

The ERDC Environmental Lab performed PFAS analysis for this project following Draft Method 1633 on their new LC-QqQ-MS. Their analysis methods are detailed in the Standard Operating Procedures and the Analytical Confirmation White Paper.

4.4 DATA REDUCTION

Data from tests using both PFAS and methylene blue show roughly exponential reductions in concentration as a function of time after the start of HC of the form $C(t) = C(t=0) \exp(-kt)$ where k is the decay rate. These data can be used to calculate the probability of destruction per pass through the orifice plate, which allows comparison of destruction efficiency across a range of test conditions. The exponential behavior implies that concentration decays according to:

$$V \frac{dC}{dt} = \dot{V} C \eta \quad (8)$$

which can be rearranged to give:

$$\frac{dC}{C} = \frac{\dot{V} \eta}{V} dt = \frac{dt}{\tau} \quad (9)$$

where V is the system volume, C is the PFOS concentration, \dot{V} is the volumetric flow rate through the orifice, η is the fraction of PFOS molecules that are removed during a single pass through the orifice, and $\tau=1/k$ is the time constant for exponential decay of the PFOS concentration. Integrating

this equation results in the observed exponential decay of concentration with time constant τ . The time constant of the decay can then be used to compute the orifice efficiency η according to:

$$\eta = \frac{V}{\tau \dot{V}} \quad (10)$$

5 RESULTS AND DISCUSSION

5.1 EVALUATE CAVITATION INTENSITY

We designed and fabricated a total of four orifice plates to use in evaluating cavitation intensity. Two had a single hole in the orifice plate, and two had seven holes arranged in a hex pattern with an additional hole in the middle. The holes were size to give $\gamma = 0.14$ and $\gamma = 0.25$ for each single and seven-hole orifice plate. Figure 7 shows the cavitation numbers achieved for each orifice plate when operating the test loop at a range of recovery pressures (the pressure after the orifice plate) and pump speeds. The photos in Figure 8 show cavitation occurring in two of the orifice plates. Consistent with expectations, we typically saw cavitation for cavitation numbers below one and no cavitation for cavitation numbers above one. Near a cavitation number of one, the cavitation was weak, and as the cavitation number decreased below one, cavitation became more intense. We found that we can achieve lower cavitation numbers with smaller orifices, lower recovery pressures, and increasing pump speed. The flow rate is a function of the pump speed and the orifice area. For the larger orifices, we were unable increase the flow rate and pressure drop across the orifice enough to get below a cavitation number of about 0.8 because of pressure drops elsewhere in the test loop, as discussed in Section 4.1. We observed similar cavitation numbers and slightly lower pressure drops across the orifice when using multiple holes in the orifice plate as compared to a single orifice with the same area.

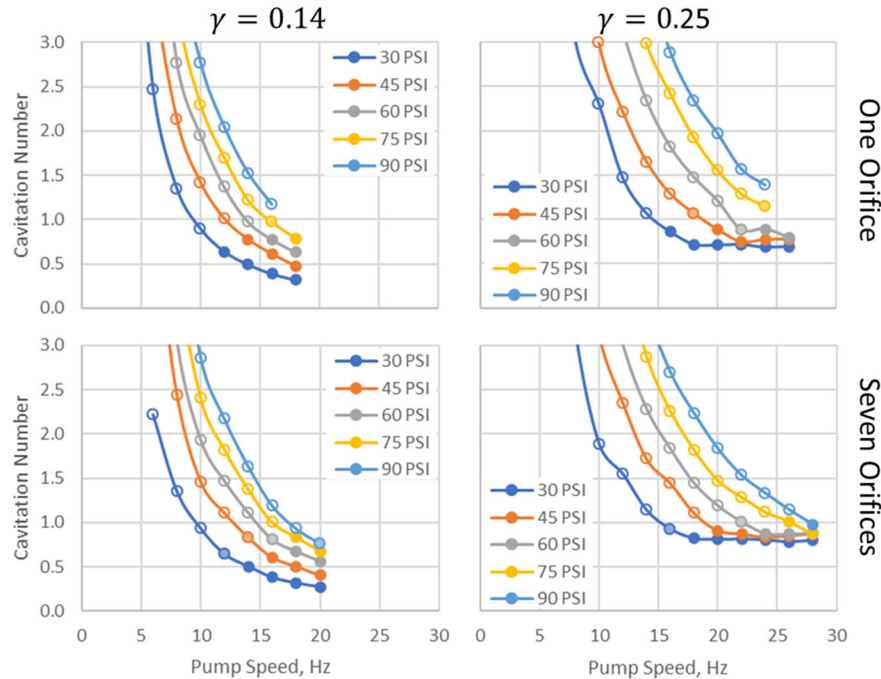


Figure 7. Experimental Conditions Tested With Distilled Water. Solid circles represent conditions with cavitation, and hollow circles represent conditions without cavitation. A cavitation number equal to one is roughly the threshold for onset of cavitation.

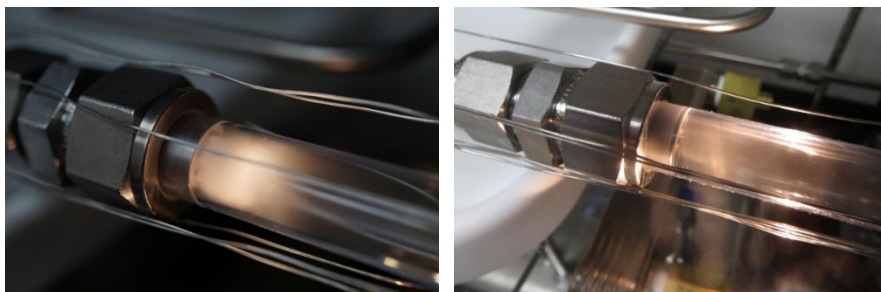


Figure 8. Photos of Cavitation in the $\gamma = 0.14$, Seven Orifice Plate and the $\gamma = 0.25$, Single Orifice Plate

5.2 EVALUATE REACTOR DESIGN AND OPERATING CONDITIONS FOR HYDROXYL RADICAL GENERATION

Hydroxyl radicals generated by HC are believed to be critical for breaking down the C–F bonds in PFAS and are thus critical to fully destroying PFAS (Vecitis et al. 2009). Because analysis of PFAS is time consuming and therefore expensive, we used methylene blue dye as a proxy to evaluate hydroxyl radical generation (Li et al. 2017). This dye is a hydroxyl scavenger that is initially a bright blue color but turns colorless upon reacting with hydroxyl ions. We implemented an in-line absorption measurement, described in Section 4.2, to monitor the methylene blue concentration during experiments. Representative absorption data and photographs from an experiment with the $\gamma = 0.14$ single hole orifice plate are shown in Figure 9. We tested a range of orifice plates and operating conditions and recorded the flow rate and pressure drop across the orifice and calculated the cavitation number and single-pass destruction efficiency for each experiment. These results are summarized in Table 1.

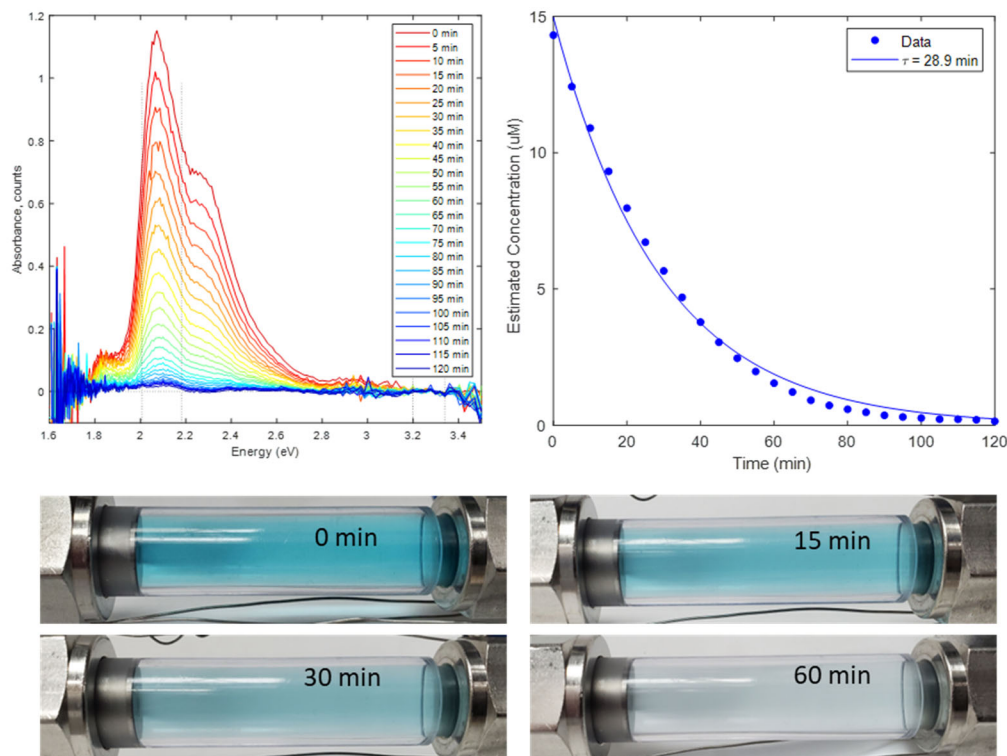


Figure 9. Absorbance Spectra, Concentration Decay Curve, and Photographs of the Orifice Plate at Select Times in an Experiment with Methylene Blue and the $\gamma = 0.14$ Single Orifice.

Table 1. Test Conditions With Methylene Blue (MB)

*Note: In these experiments, cavitation may also have occurred in a valve (V2) in the test loop (see Section 4.1 for details)

# Holes	γ	MB:H ₂ O ₂ Molar Ratio	Pump Speed (Hz)	Recovery Pressure (psia)	Flow Rate (LPM)	Ca	Decay Time (min)	Single Pass Efficiency
1	0.14	-	18	30	15	0.32	28.9	0.083%*
7	0.14	-	18	30	16	0.32	25.0	0.090%*
7	0.25	-	28	75	28	0.87	15.2	0.086%*
19	0.14	-	18	25	15	0.30	39.0	0.065%
19	0.14	-	22	43	18	0.36	22.0	0.097%
19	0.14	-	26	58	21	0.35	17.5	0.103%
19	0.10	1:50	22	59	12.5	0.58	20.3	0.150%
19	0.10	1:100	22	56	12.5	0.56	20.8	0.146%
19	0.10	1:200	22	60	12.5	0.60	19.9	0.153%

Number of Orifices. We initially compared the methylene blue degradation rates of two orifice plates with the same total orifice area ($\gamma = 0.14$), but one had a single hole whereas the other had seven holes. We found that under the same operating conditions, the plate with seven orifice holes gave a higher single pass efficiency while also having lower pressure drop across the orifice. Thus, increasing the number of orifices for a given total open flow area improves hydroxyl radical generation while reducing the required pump head.

Total Orifice Area. We then compared the $\gamma = 0.14$ seven-hole orifice to a $\gamma = 0.25$ seven-hole orifice. The larger area orifice plate allowed for a higher flow rate and produces a smaller pressure drop. However, it was harder to achieve low cavitation numbers and high pressure drops across other elements in the system loop at high flow rates. As a result, the larger open flow area orifice plate performed worse than the smaller plate. Further discussion of the issues with our test loop that this experiment uncovered are discussed in Section 4.1.

Recovery Pressure. Next, we measured the effects of recovery pressure on orifice plate performance. For these experiments, we used a 19-hole orifice plate with $\gamma = 0.14$. Achieving the same cavitation number of about 0.3 to 0.36 while increasing the recovery pressure requires using higher flow rates. We found that the single pass efficiency increased when increasing the recovery pressure from 25 psia to 60 psia. Unfortunately, the pump operation was not stable for long periods of time at 60 psia, and we could not push the recovery pressure higher with this orifice plate due to system limitations described in Section 4.1.

Oxidizing Agent. Finally, we decided to add hydrogen peroxide (H₂O₂) as an oxidant to increase the production of •OH. For these experiments, we also made a smaller 19-hole orifice plate with $\gamma = 0.1$ so that we could achieve lower cavitation numbers at a recovery pressure of 60 psia while staying within the stable operating limits of the pump. We tested methylene blue to H₂O₂ molar ratios of 1:50, 1:100, and 1:200 and found similar results in all three cases, with slight variations explained by slight differences in the recovery pressure. Unfortunately, due to time

constraints we were not able to conduct the control experiment without H₂O₂ with this orifice at these operating conditions. However, the single pass efficiency of 0.15% in these experiments was at least 50% higher than that in all other experiments. It seems unlikely that this increase is due to the orifice geometry and operating conditions alone, and we attribute it to the presence of H₂O₂.

5.3 EVALUATE PFAS DESTRUCTION

We chose PFOS as a representative PFAS chemical for initial testing and measured destruction rates at four different test conditions: (1) PFOS in distilled water at 20°C, (2) PFOS in distilled water with H₂O₂ in a 1:50 F atom:H₂O₂ molar ratio, (3) PFOS in distilled water using HCl to lower the pH to 4, and (4) PFOS in distilled water at 40°C. All experiments were conducted using the $\gamma = 0.1$, 19-hole orifice plate with a recovery pressure of 60 psia, a pump speed of 22 Hz, and a flow rate of 12.5 LPM, and all except (4) were conducted at 20°C. Each experiment ran for four hours. We present both the raw data and data that have been corrected for the fact that 9 mL (5 mL discard plus two 2 mL samples) were removed from the 600 mL sample volume at each time point in Figure 10.

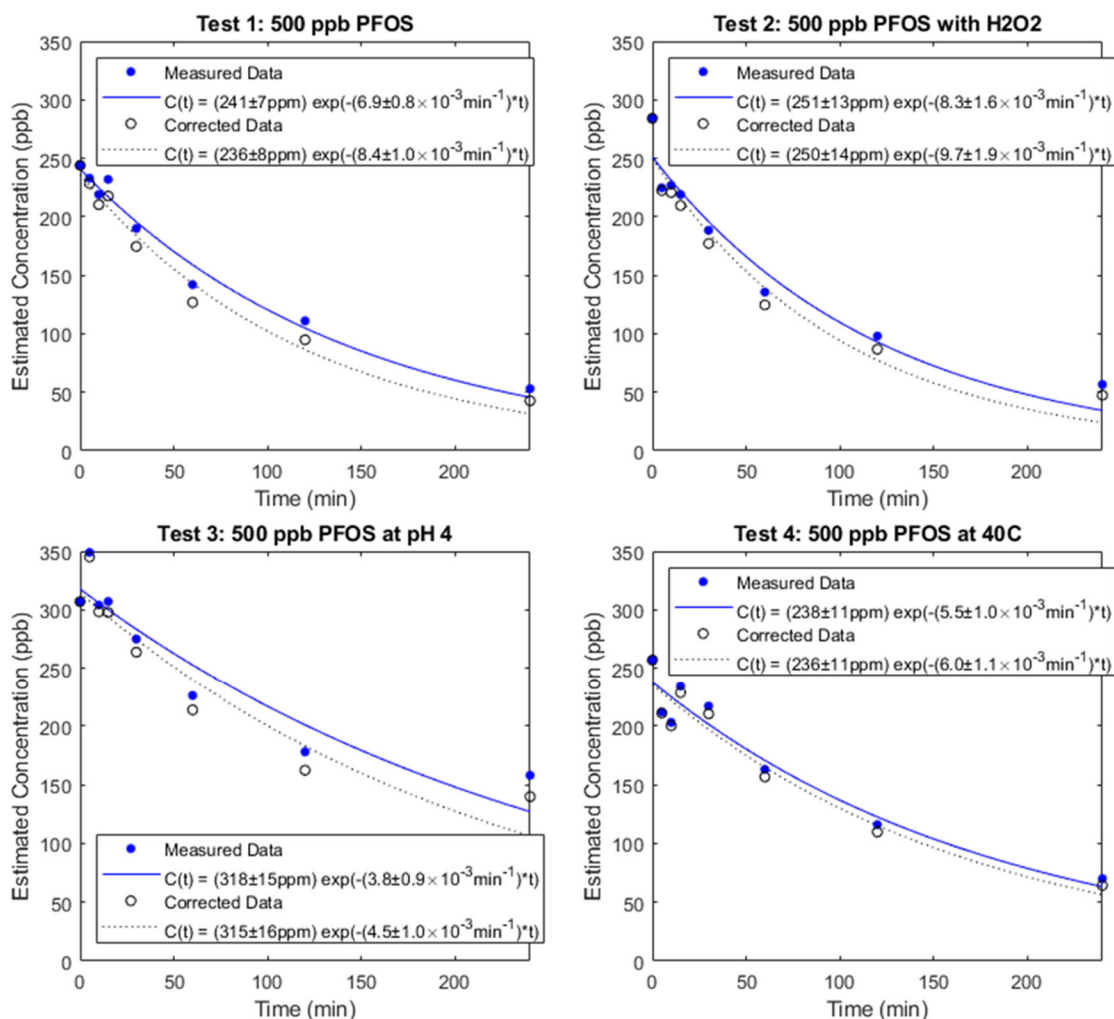


Figure 10. Experimental Results From Testing With PFOS

We observed that adding H_2O_2 increased the single pass efficiency by about 20% from 0.025% to 0.030%, indicating that the presence of additional hydroxyl groups improves the destruction rate, consistent with observations with other pollutants in Gagol et al. (2018) and Tao et al. (2016). Reducing the pH from neutral to a pH of 4 decreased the single pass efficiency, contrary to the observations in Gole (2018) for sonochemical degradation. Operating at a higher temperature of 40°C also reduced the destruction efficiency. While a higher temperature should assist in defluorination (Trang et al. 2022), it also results in an approximate doubling of the water vapor pressure and density that would act to slow down bubble collapse and reduce the cavitation intensity.

Our initial PFOS experiments showed that HC can destroy PFOS, but because of the relatively slow degradation rates in our bench-scale system, at least 50 ppb ($\sim 10\%$ of the initial concentration) remained at the end of the four-hour experiment. We thus decided to run a longer, 24-hour experiment (Figure 11). We repeated the conditions from the first test (~ 500 ppb PFOS, 20°C , 60 psia recovery pressure), but the observed decay was about three to four times slower. Following the experiment, we investigated possible causes for the slower decay rate and realized that black debris was stuck to the insides of the orifice holes and partially blocking two holes (Figure 12). This debris would reduce the flow rate through the orifice and change how fluid is accelerated through the holes, potentially reducing the intensity of the resulting cavitation. Unfortunately, the flow meter must be read manually, and it was not recorded at later times during the experiment. The debris likely originated from the pump wear plates and bearings. We thought this wear would be negligible at our operating conditions (see Section 4.1), but this was not so for this longer experiment. We also went back and looked at the pressure drop across the orifice during this experiment and found that it increased by about 10 psi over the 24-hour period, further supporting the idea that this debris built up over time and blocked the orifice. Reviewing the pressure drop in previous experiments suggests that debris may also have been an issue in the 40°C experiment and to a lesser extent in the H_2O_2 and pH 4 experiments. Average pressures at different locations in the system are given in Table 2.

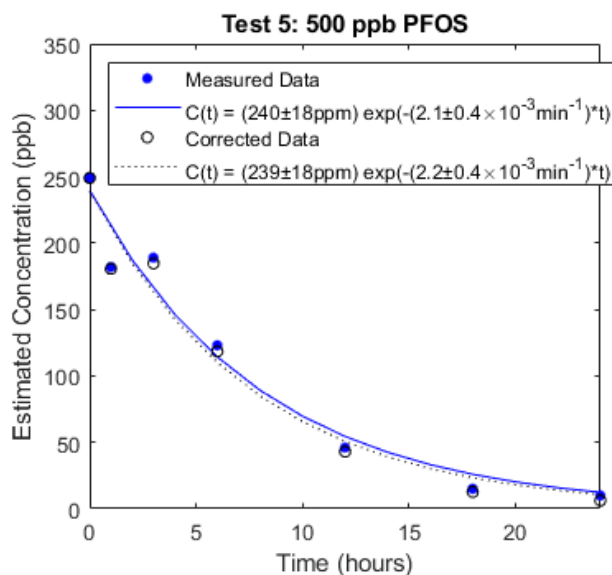


Figure 11. Experimental Results From 24-Hour Test With PFOS



Figure 12. Photos of Orifice Plate at Conclusion of Testing With PFOS

Table 2. Average Operating Conditions During PFOS Experiments				
Test	Pressure Before Orifice (psia)	Pressure After Orifice (psia)	Pressure Before Pump (psia)	Temperature (°C)
1: PFOS at 20°C	164.8	59.8	52.3	19.8
2: PFOS with H ₂ O ₂	173.5	58.9	51.8	19.4
3: PFOS at pH 4	173.9	59.9	52.5	19.4
4: PFOS at 40°C	188.3	60.3	52.9	39.3
5: PFOS 24 hr exp't	186.6	59.4	51.9	19.6

5.4 BYPRODUCTS OF PFAS DESTRUCTION

In our PFAS analysis, we looked for shorter-chain PFAS chemicals that might be expected to be breakdown products of PFOS. The measured concentrations of these chemicals at the conclusion of our four-hour experiments are presented in Figure 13, and a comparison of the four and 24-hour tests is presented in Figure 14. We also analyzed the fluoride concentration at the conclusion of each experiment, and results are presented in Table 3. Of the four-hour tests, PFOS without chemical additives had the most complete breakdown, as indicated by the highest free fluoride concentration and lowest PFOS and shorter-chain PFAS concentrations. The fractions of the recovered fluoride that was fluoride ions, short chain PFAS, and remaining PFOS were approximately the same at 20°C and 40°C. The addition of hydrogen peroxide as an oxidant had a minimal effect on the degradation rate and byproducts produced. Acidic conditions (pH 4) noticeably inhibited PFOS breakdown. Running the 20°C experiment with no chemical additives for a longer time resulted in more free fluoride ions, similar concentrations of shorter-chain sulfonic acids, and higher concentrations of carboxylic acids. Whether the higher concentration of carboxylic acids is due to the debris on the orifice holes affecting cavitation conditions or to an inherent reduced efficiency on carboxylic acid PFAS as compared to sulfonic acid PFAS is an

open question that should be addressed in future work. However, chemical additives such as persulfate have been shown to be effective at destroying PFOA (Leung 2022), and these could be added to the HC reactor to improve the carboxylic acid PFAS destruction efficiency if needed.

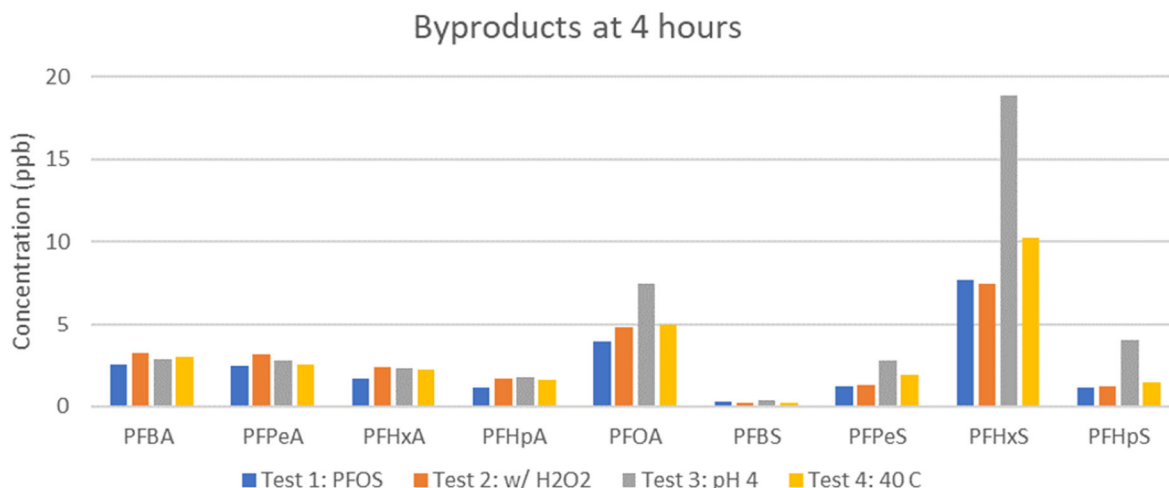


Figure 13. Byproducts of PFOS Degradation After 240 Minutes in the HC Reactor. Byproducts are arranged in order of increasing molecular weight for carboxylic acids (PFxA) and then sulfonic acid (PFxS) where x indicates the carbon chain length from 4 (butane) to 8 (octane).

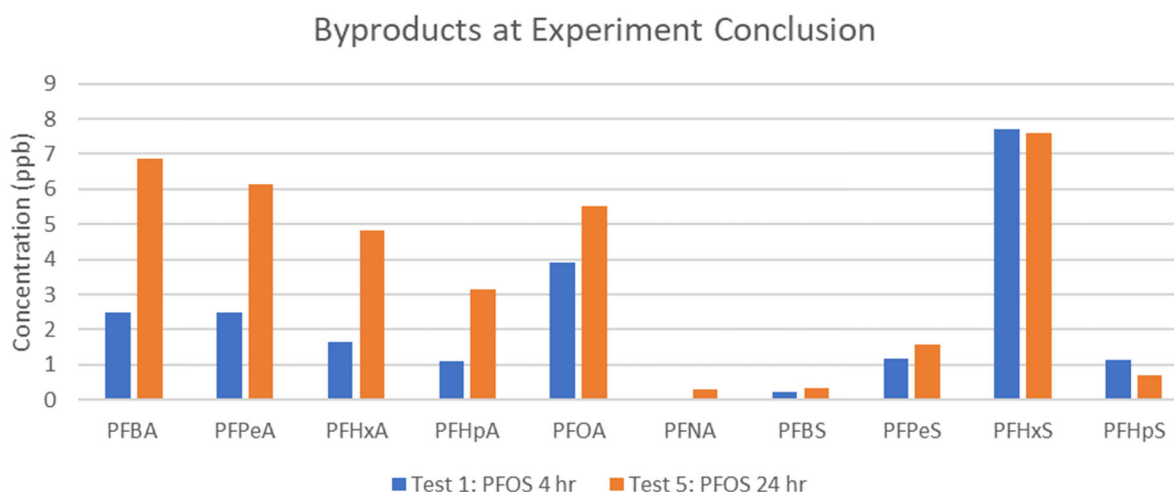


Figure 14. Byproducts of PFOS Degradation at the End of a 4-Hour and a 24-Hour Experiment in the HC Reactor. Byproducts are arranged in order of increasing molecular weight for carboxylic acids (PFxA) and then sulfonic acid (PFxS) where x indicates the carbon chain length from 4 (butane) to 9 (nonane).

The presence of shorter-chain sulfonic and carboxylic acids in our experiments differs from the results of the sonochemical PFOS degradation experiments described by Vecitis et al. (2008), which detected no shorter-chain perfluoro-acid intermediate products, and observed SO_4^{2-} as the only sulfur-containing product. The first step of the mechanism proposed by Vecitis et al. (2008) and described in Section 3.2 is the cleavage of the sulfonic head group; they include no mechanism that allows for the formation of shorter-chain sulfonic acids or of carboxylic acids from PFOS. In

contrast, Rodriguez-Freire et al. (2015) monitored fluoride and sulfate ion concentrations during sonochemical cavitation experiments with PFOS and found that defluorination occurred at higher rates than cleavage of the sulfonic head group. They hypothesize that shorter-chain fluorinated sulfonates may be formed as reaction products. Moriwaki et al. (2005) did observe C6 and C7 sulfonic acids and C2 to C7 carboxylic acids in sonochemical cavitation experiments with PFOS. They hypothesize that PFOA may be formed by oxidation after cleavage of the sulfate group, and the shorter-chain acids could be formed by either sequential dissociation of CF_2 from longer-chain acids, or by cleavage of the carboxyl group followed by oxidation of the perfluorocarbon to form shorter-chain carboxylic acids or recombination with SO_3^- to form shorter-chain sulfonic acids. The cleavage steps likely occur via pyrolysis at the bubble interface, and the oxidation occurs by reaction with hydroxyl radicals in the aqueous phase. Taken together, these sonochemical degradation experiments indicate that different degradation mechanisms may be dominant under differing cavitation conditions. The presence of shorter-chain sulfonic and carboxylic acids indicates that the degradation mechanisms in our experiments may have been more similar to those observed by Rodriguez-Freire et al. (2015) and Moriwaki et al. (2005). However, because we did not simultaneously monitor for the sulfate ion and the presence of fluoroalkanes and fluoroalkenes or de-fluorinated hydrocarbons, we cannot definitively say whether both mechanisms may have been present. In future work, we plan to expand our analytical techniques to better capture more of these possible reaction products.

Table 3. Fluorine Measured After HC Reactor Experiment Conclusion (Four or Twenty-Four Hours) All units in $\mu\text{g/L}$ (ppb) fluorine			
Test	Fluoride Ions	Other Byproducts	Remaining PFOS
1: PFOS at 20°C	170.9	20.9	34.2
2: PFOS with H_2O_2	145.2	24.5	36.6
3: PFOS at pH 4	121.9	38.3	102.0
4: PFOS at 40°C	247	26.5	45.1
5: PFOS 24 hr exp't	531	38.6	6.5

Table 4. Measured PFOS Concentrations from Samples Taken During Experiment Setup All units in $\mu\text{g/L}$ (ppb) PFOS					
Test	Stock Solution	Inlet Tank	After Fill, Before Degas	Concentration at Time 0	Total Recovered Fluoride PFOS Equivalent
1: PFOS at 20°C	562	N/A	269	244	350
2: PFOS with H_2O_2	478	400	N/A	284	319
3: PFOS at pH 4	537	604	N/A	307	406
4: PFOS at 40°C	341	N/A	267	257	493
5: PFOS 24 hr exp't	368	812	396	249	892

Table 4 presents PFOS concentrations measured at various points during experimental setup and compares them to the PFOS-equivalent total fluoride recovered at the conclusion of the

experiment. The stock solution sample was taken directly from the high-density polyethylene bottle with polypropylene cap before it was added to the inlet tank. The inlet tank sample was taken from the remaining solution in the stainless steel inlet tank at the conclusion of the experiment. The after-fill sample was taken after filling the system, including the degasser side loop, by running the pump at 2 Hz for a few minutes. The concentration at time 0 was taken after degassing, which involved running the pump at 2 Hz at a recovery pressure of 15 psia, then at 4 and 6 Hz at 30 psia recovery pressure, and 8 and 10 Hz with a brief (~15 s) spike up to 18 Hz at a recovery pressure of 60 psia to dislodge any stuck bubbles. With the exception of the brief spike to 18 Hz, these conditions do not cause cavitation in the orifice, and each pump speed is held for about two minutes. The total recovered fluoride PFOS equivalent gives the amount of PFOS that would yield the total quantity of fluoride ions detected in the fluoride ions, shorter-chain PFAS byproducts, and remaining PFOS at the conclusion of the experiment. We note that our detection methods do not include C1, C2, and C3 fluorocarbons, which is a weakness in our ability to close the fluorine mass balance.

We notice concerning trends in the data in Table 4 that suggest PFOS may adhere to surfaces somewhere in our system and be slowly re-dissolved throughout the course of the experiment. In the first test, the fill and time-zero samples were significantly lower than the stock solution concentration, but the total fluoride recovered indicates that more PFOS was broken down than was measured in the fill or time-zero samples. The same is true for the time zero and final samples in the second and third tests, and by the fourth and fifth test, the final concentration is substantially higher than the stock, fill, or time zero concentrations. These results indicate that PFOS is being adsorbed and then released somewhere within the main system loop (i.e. not in the degasser, see Figure 3). Additionally, the concentration measured in the inlet tank is below the stock solution in the second test, slightly above in the third test, and well above by the fifth test. The inlet tank is stainless steel, so PFOS adsorbing to the walls is unlikely (to the best of our knowledge). This implies that our cleaning procedures between tests may not be adequate and may be leaving residual PFOS in the tank that redissolves into solution during the next test. While we attempted to design our experimental setup and cleaning procedures to avoid issues with PFOS adsorption and contamination from experiment to experiment, clearly some issues remain that will need to be resolved in future work. In particular, we had hoped to avoid using organic solvents for cleaning, but our initial results indicate that it is needed, and we will modify our procedures going forward to test using either a methanol rinse or an acetone and isopropanol rinse before doing a final water rinse. These issues currently complicate the interpretation of results and the ability to close the fluorine mass balance. In particular, the decay rates shown in Figure 10 and Figure 11 may appear slower than the true PFOS decay rate if additional PFOS is dissolving into solution during the experiment. The total fluoride recovered at the end of Test 1 was only 62% of that present in the stock solution, and of what was recovered, 76% of it was fully broken down to fluoride ions. In contrast, the total fluoride-containing compounds recovered was 240% of that in the stock solution, and of what was recovered, 92% was fully broken down to fluoride ions.

5.5 ANALYZE SCALABILITY

Data from the HC reactor tests enable us to make some very rough and preliminary estimates of how the process can be used to destroy PFAS in the field. These extrapolations are useful mainly for order-of-magnitude estimations due to limitations in our initial HC reactor, which prevented us from exploring a wide range of HC conditions. First, we were not able to

operate at as high of recovery pressures and flow rates as we would have liked. Second, we experienced some clogging of the orifice that increased the pressure drop, reduced the flow rate, and may have had other unintended effects on the bubble formation and collapse. Third, the system seems to absorb some PFOS and then rerelease it throughout the experiments, slowing the observed decay rate by an unknown amount. These problems are all surmountable with careful redesign of the system and experimental procedures, but they make it challenging to analyze the scalability or commercial viability at this time. We also note that to date we have tested only with PFOS at a single concentration; the PFAS decay rate may also depend on the PFAS concentration, types of PFAS (chain length, head group, etc.) in the waste stream, and any other co-contaminants present. Further research into these effects is also needed and described in the next section. At this time, we perform only a basic analysis of potential system sizes below, and we consider the effects of the observed rate of PFAS destruction and an increase of one to two orders of magnitude when sizing a potential system.

We can estimate the number of passes, x , through the orifice required to destroy PFAS as:

$$x = \frac{\ln(C_f/C_i)}{\ln(1-\eta)} \quad (11)$$

where C_i is the initial PFAS concentration, C_f is the final desired concentration, and η is the single pass destruction efficiency. The required flow rate, Q , through a treatment system loop is then given by:

$$Q = \frac{Vx}{t} \quad (12)$$

where t is the time it takes to treat a volume V . We consider three possible PFAS treatment scenarios: (1) 50 ppt PFAS in a ground water source for a home using 150 gallons of water per day (GRACE), (2) AFFF with 6% PFAS in a 55-gallon drum, and (3) 200 ppt PFAS in a surface pond with a ~6 million gallon volume (0.8 m deep, 7.1 acre surface area) (Hinkle 2021; Eichner et al. 2008). In all cases, we wish to reduce the PFAS concentration to below the 12 to 15 ppt NH regulatory limit. Potential treatment scenarios and the required pump flow rates are given in Table 5. The current maximum observed single-pass efficiency of 0.03% would require relatively large pumps or long treatment times, but an improvement of one or two orders of magnitude in the single-pass efficiency reduces these to reasonable flow rates and treatment times. Achieving one or two orders of magnitude of improvement should be possible with improved operating conditions and improved cavitation reactor design. In particular, rotor hydrodynamic reactors generally have much higher cavitation efficiency than conventional orifice plate or venturi cavitation reactors (Song et al. 2022) and are a promising avenue for future development.

Table 5. Potential PFAS Treatment Scenarios

Scenario	Treatment Volume	Treatment Time	Single Pass Efficiency (%)	Concentration Reduction	Pump Flow Rate Required (gpm)
1: Home	150 gal	1 day	0.03%	10x	171 gpm
1: Home	150 gal	1 day	0.3%	10x	17 gpm
1: Home	150 gal	1 day	0.3%	100x	34 gpm
2: AFFF	55 gal	30 days	0.03%	10 ¹⁰ x	98 gpm
2: AFFF	55 gal	7 days	0.3%	10 ¹⁰ x	42 gpm
2: AFFF	55 gal	1 day	0.3%	10 ¹⁰ x	293 gpm
3: Pond	6E+06 gal	365 days	0.03%	10x	87,600 gpm
3: Pond	6E+06 gal	365 days	0.3%	10x	8,750 gpm
3: Pond	6E+06 gal	365 days	3%	10x	863 gpm
3: Pond	6E+06 gal	365 days	3%	100x	1,730 gpm

6 CONCLUSIONS AND IMPLICATIONS FOR FUTURE RESEARCH/IMPLEMENTATION

This limited-scope project successfully met the project objectives and demonstrated that hydrodynamic cavitation is a feasible technology for destruction of PFAS. Specifically, we found that:

1. HC destroys PFOS across the range of conditions that we tested. Destruction efficiencies were on the order of 0.025% per pass under all conditions tested. Adding H₂O₂ to the PFOS solution increased the destruction efficiency to 0.030% per pass, while reducing the pH or running at higher temperature decreased the destruction efficiency. Using methylene blue as a proxy, we also showed that multiple orifice holes, smaller total orifice area, and higher recovery pressure increase the destruction efficiency.
2. A majority of the PFOS is fully broken down to yield fluoride ions, though small concentrations of shorter-chain PFAS (sulfonic and carboxylic acids) are also present. Adding H₂O₂, reducing the pH, and increasing the temperature all increased the concentration of shorter-chain PFAS. We were not able to demonstrate that longer operation could fully destroy all PFOS and shorter-chain PFAS byproducts due to limitations in our current experimental setup. However, it seems probable that full destruction is possible based on the low concentrations at the conclusion of the longer experiment.
3. It appears to be feasible to use HC technology to destroy PFAS in the field in a variety of applications, including residential water treatment, destroying stored AFFF, and remediating natural bodies of water. With the current destruction efficiency, flow rates may be large or treatment times long, but improvements of one or two orders of

magnitude in the destruction efficiency should be feasible with further development and will greatly improve the required treatment times and flow rates.

While this initial demonstration of hydrodynamic cavitation to destroy PFOS is promising, we encountered several challenges that should be addressed in near-term follow-on R&D:

1. Upgrade the pump in the HC reactor to a model that can achieve high flow rates and low cavitation numbers at high recovery pressures. Our results to date indicate that these operating conditions would generate cavitation conditions that would be most successful at destroying PFAS, and likely increase the degradation rates. Additionally, the new pump will avoid the problematic wear and debris issues and possible adsorption of PFAS that complicated interpreting our results during this initial study. We have identified a suitable pump, but it has a ~5-month lead time that will need to be accounted for in the project schedule.
2. Identify and eliminate materials that may accumulate PFAS, such as the degasser, pump, and potentially others. Investigate whether stainless steel is adsorbing and rereleasing PFAS during the experiments. Also redesign the system to incorporate all components, including the inlet tank, water trap, and degassing into the main system loop so that all wetted surfaces are treated during system operation.
3. Enhance cleaning methods using organic solvents to eliminate PFAS hold-up between tests and improve mass balance measurements.
4. Improve analytical methods to improve the fluorine mass balance. Use gas chromatography-mass spectrometry to measure volatile products of PFAS destruction, and combustion measurements of total organic fluorine concentration. Also measure the sulfate ion concentration and total organic carbon to aid in differentiating between possible destruction mechanisms.

Once these experimental challenges have been addressed, we recommend additional R&D to further develop this technology and assess its suitability for specific applications. The overall objectives of this phase of the research program would be to improve the HC efficiency and demonstrate its effectiveness against a wider array of PFAS-contaminated matrices:

1. Study varying PFOS concentrations and observe how the destruction efficiency varies with concentration. PFAS are surfactants and are expected to preferentially assemble at the bubble interface. At high PFAS concentrations, the bubble surfaces may become saturated, and so the degradation rate may depend on the number of available interfacial sites, rather than the PFAS concentration. Additionally, high concentrations could lower the interfacial tension of water and affect the formation and collapse of bubbles, potentially reducing the temperatures and pressures achieved and thus the destruction efficiency. The number of available interfacial sites and the intensity of bubble collapse will vary with cavitation conditions, so these concentration-dependent measurements should be conducted under multiple reactor configurations. Study both very low concentrations (ppt) to confirm whether HC can fully degrade PFOS and high concentrations approaching those in AFFF concentrates and rinsates to investigate whether HC might be suitable for disposing of AFFF stockpiles.

2. Compare degradation rates for PFAS with different length carbon backbones or other head groups (carboxylic acids). These degradation rates will also have important implications for the breakdown of any shorter-chain intermediates that are generated.
3. Consider the effects of co-contaminants that may be present in matrices of interest such as AFFF, wastewater streams, and/or groundwater. These might include other surfactants, hydrocarbons, alcohols, minerals, and ions. HC has been shown to destroy a range of organic compounds and bacteria, so co-degradation of multiple contaminants could be a desirable feature of this technique. Alternatively, co-contaminants may interfere with bubble formation and collapse, compete for interfacial sites, or compete for hydroxyl radicals, all slowing the rate of degradation.
4. Research new HC reactor designs, specifically looking non-passive systems (including high-speed rotors, for example (Song et al. 2022)) that may be able to give orders of magnitude efficiency improvements. These studies would involve both CFD simulations and experimental validation of the most promising design(s), and could occur either simultaneously or sequentially with the experiments on different PFAS-contaminated matrices.

The experiments described above will help determine the most appropriate PFAS-contaminated matrices for treatment with HC and the destruction efficiencies that may be achieved for each. Based on these results, we could then identify suitable applications for field demonstration(s) and successful scale-up of the technology. Long-term results of a successful program will be the deployment of mobile and/or stationary HC facilities that support cost-effective and efficient remediation of PFAS-contaminated sites.

7 LITERATURE CITED

- Bandala, E. R. and Rodriguez-Narvaez, O. M., “On the Nature of Hydrodynamic Cavitation Process and Its Application for the Removal of Water Pollutants,” *Air, Soil and Water Research*, Vol. 12, 2019, doi: 1178622119880488.
- Beitsch, R., “Defense Department Says ‘Forever Chemical’ Cleanup Costs Will Dwarf Earlier Estimates,” *The Hill*, 9/12/2019, <https://thehill.com/policy/energy-environment/461171-dod-says-forever-chemical-cleanup-costs-will-dwarf-earlier> (cited March 5, 2020).
- Braeutigam, P., Franke, M., Wu, Z. L. and Ondruschka, B., “Role of Different Parameters in the Optimization of Hydrodynamic Cavitation,” *Chemical Engineering & Technology: Industrial Chemistry-Plant Equipment-Process Engineering-Biotechnology*, Vol. 33, No. 6, 2010, pp. 932–940.
- Burzio, E., Bersani, F., Caridi, G. C., Vesipa, R., Ridolfi, L. and Manes, C., “Water Disinfection by Orifice-Induced Hydrodynamic Cavitation,” *Ultrasonics Sonochemistry*, 2019, p. 104740.
- Campbell, T. Y., Vecitis, C. D., Mader, B. T. and Hoffmann, M. R., “Perfluorinated Surfactant Chain-Length Effects on Sonochemical Kinetics,” *The Journal of Physical Chemistry A*, Vol. 113, No. 36, 2009, pp. 9834–9842.

- Campbell, T. and Hoffmann, M. R., “Sonochemical Degradation of Perfluorinated Surfactants: Power and Multiple Frequency Effects,” *Separation and Purification Technology*, Vol. 156, 2015, pp. 1019–1027.
- Capocelli, M., Musmarra, D., Prisciandaro, M. and Lancia, A., “Chemical Effect of Hydrodynamic Cavitation: Simulation and Experimental Comparison,” *AIChE Journal*, Vol. 60, No. 7, 2014a, pp. 2566–2572.
- Capocelli, M., Prisciandaro, M., Lancia, A. and Musmarra, D., “Hydrodynamic Cavitation of P-Nitrophenol: A Theoretical and Experimental Insight,” *Chemical Engineering Journal*, Vol. 254, 2014b, pp. 1–8.
- Cappa, O. A., Soeira, T. V., Simões, A. L., Junior, G. B., and Gonçalves, J. C., “Experimental and Computational Analyses for Induced Cavitating Flows in Orifice Plates,” *Brazilian Journal of Chemical Engineering*, 2020, pp. 1–11.
- Cheng, J., Vecitis, C. D., Park, H., Mader, B. T. and Hoffmann, M. R., “Sonochemical Degradation of Perfluorooctane Sulfonate (PFOS) and Perfluorooctanoate (PFOA) in Landfill Groundwater: Environmental Matrix Effects,” *Environmental Science & Technology*, Vol. 42, No. 21, 2008, pp. 8057–8063.
- Eichner, E., Cambareri, T. C., McCaffery, D., Belfit, G. and Wu, X., “Barnstable Ponds: Current Status, Available Data, and Recommendations for Future Activities,” Final Report for the Town of Barnstable Conservation Division, July 2008, <https://tobweb.town.barnstable.ma.us/departments/Conservation/Wequaquet/WeqInBarnstablePonds2008Report.pdf> [cited November 14, 2022].
- Environmental Working Group and the Social Science Environmental Health Research Institute at Northeastern University (EWG), https://www.ewg.org/interactive-maps/2019_pfas_contamination/map/ [cited January 7, 2020].
- Fernandez, N. A., Rodriguez-Freire, L., Keswani, M. and Sierra-Alvarez, R., “Effect of Chemical Structure on the Sonochemical Degradation of Perfluoroalkyl and Polyfluoroalkyl Substances (PFASs),” *Environmental Science: Water Research & Technology*, Vol. 2, No. 6, 2016, pp. 975–983.
- Gągol, M., Przyjazny, A. and Boczkaj, G., “Wastewater Treatment by Means of Advanced Oxidation Processes Based on Cavitation—A Review,” *Chemical Engineering Journal*, Vol. 338, 2018, pp. 599–627.
- Gogate, P. R. and Bhosale, G. S., “Comparison of Effectiveness of Acoustic and Hydrodynamic Cavitation in Combined Treatment Schemes for Degradation of Dye Wastewaters,” *Chemical Engineering and Processing: Process Intensification*, Vol. 71, 2013, pp. 59–69.
- Gole, V. L., Fishgold, A., Sierra-Alvarez, R., Deymier, P. and Keswani, M., “Treatment of Perfluorooctane Sulfonic Acid (PFOS) Using a Large-Scale Sonochemical Reactor,” *Separation and Purification Technology*, Vol. 194, 2018, pp. 104–110.
- GRACE Communications Foundation, “Water Footprint Calculator,” <https://www.watercalculator.org/footprint/indoor-water-use-at-home/> [cited November 14, 2022].

- Hinkle, J., “PFAS Contamination: Of 21 Barnstable Ponds Tested, 21 Had Contaminants, Town Report Finds,” *Cape Cod Times*, October 4, 2021. <https://www.capecodtimes.com/story/news/2021/10/04/pfas-pollution-cape-cod-banstable-ponds-tested-all-contaminated/5903184001/> [cited November 14, 2022].
- Hu, X. C., Andrews, D. Q., Lindstrom, A. B., Bruton, T. A., Schaider, L. A., Grandjean, P. et al., “Detection of Poly- and Perfluoroalkyl Substances (PFASs) in U.S. Drinking Water Linked to Industrial Sites, Military Fire Training Areas, and Wastewater Treatment Plants,” *Environ. Sci. Technol. Lett.*, Vol. 3, No. 10, 2016, pp. 344–350.
- ITRC PFAS Fact Sheets, <https://pfas-1.itrcweb.org/fact-sheets/> [cited March 5, 2020].
- Kanthale, P. M., Gogate, P. R., Pandit, A. B. and Wilhelm, A. M., “Dynamics of Cavitation Bubbles and Design of a Hydrodynamic Cavitation Reactor: Cluster Approach,” *Ultrasonics Sonochemistry*, Vol. 12, No. 6, 2005, pp. 441–452.
- Krishnan, J. S., Dwivedi, P. and Moholkar, V. S., Numerical Investigation Into the Chemistry Induced by Hydrodynamic Cavitation,” *Industrial & Engineering Chemistry Research*, Vol. 45, No. 4, 2006, pp. 1493–1504.
- Kumar, P., Khanna, S. and Moholkar, V. S., “Flow Regime Maps and Optimization Thereby of Hydrodynamic Cavitation Reactors,” *AIChE Journal*, Vol. 58, No. 12, 2012, pp. 3858–3866.
- Leung, S. C. E., Shukla, P., Chen, D., Eftekhari, E., An, H. Zare, F., Ghasemi, N., Zhang, D. Nguyen, N.-T. and Li, Q., “Emerging Technologies for PFOS/PFOA Degradation and Removal: A Review,” *Science of the total Environment*, Vol. 827, 153669, 2022, pp. 1–34.
- Li, X., Huang, B., Chen, T., Liu, Y., Qiu, S. and Zhao, J., “Combined Experimental and Computational Investigation of the Cavitating Flow in an Orifice Plate With Special Emphasis on Surrogate-Based Optimization Method,” *Journal of Mechanical Science and Technology*, Vol. 31, No. 1, 2017, pp. 269–279.
- Merouani, S., Hamdaoui, O., Rezzgui, Y. and Guemini, M., “Theoretical Estimation of the Temperature and Pressure Within Collapsing Acoustical Bubbles,” *Ultrasonics Sonochemistry*, Vol. 21, 2014, pp. 53–59.
- Metcalf, M., et al., “Evaluation of PFAS Treatment for Wells 2, 3, 7, and 8, Merrimack Village District (MDV), Merrimack, NH,” Underwood Engineers, December 2018. <http://www.mvdwater.org/wp-content/uploads/2018/12/PFAS-Treatment-Feasibility-Report-237-8-Final.pdf>.
- Moholkar, V. S. and Pandit, A. B., “Bubble Behavior In Hydrodynamic Cavitation: Effect Of Turbulence,” *AIChE Journal*, Vol. 43, No. 6, 1997, pp. 1641–1648.
- Moholkar, V. S., Kumar, P. S. and Pandit, A. B., “Hydrodynamic Cavitation for Sonochemical Effects,” *Ultrasonics Sonochemistry*, Vol. 6, No. 1-2, 1999, pp. 53–65.
- Moholkar, V. S., and Pandit, A. B., “Modeling of Hydrodynamic Cavitation Reactors: a Unified Approach,” *Chemical Engineering Science*, Vol. 56, 2001, pp. 6295–6302.
- Moriwaki, H., Takagi, Y., Tanaka, M., Tsuruho, K., Okitsu, K. and Maeda, Y., “Sonochemical Decomposition of Perfluorooctane Sulfonate and Perfluorooctanoic Acid,” *Environmental Science & Technology*, Vol. 39, No. 9, 2005, pp. 3388–3392.

- Pawar, S. K., Mahulkar, A. V., Pandit, A. B., Roy, K. and Moholkar, V. S., “Sonochemical Effect Induced by Hydrodynamic Cavitation: Comparison of Venturi/Orifice Flow Geometries,” *AIChE Journal*, Vol. 63, No. 10, 2017, pp. 4705–4716.
- Rodriguez-Freire, L., Balachandran, R., Sierra-Alvarez, R. and Keswani, M., “Effect of Sound Frequency and Initial Concentration on the Sonochemical Degradation of Perfluorooctane Sulfonate (PFOS),” *Journal of Hazardous Materials*, Vol. 300, 2015, pp 662–669.
- Ropeik, A., “N.H. Approves Unprecedented Limits For PFAS Chemicals In Drinking Water,” <https://www.nhpr.org/post/nh-approves-unprecedented-limits-pfas-chemicals-drinking-water#stream/0> (cited March 5, 2020).
- Sharma, A., Gogate, P. R., Mahulkar, A. and Pandit, A. B., “Modeling of Hydrodynamic Cavitation Reactors Based on Orifice Plates Considering Hydrodynamics and Chemical Reactions Occurring in Bubble,” *Chemical Engineering Journal*, Vol. 143, No. 1-3, 2008, pp. 201–209.
- Song, Y., Hou, R., Zhang, W. and Liu, J., “Hydrodynamic Cavitation as an Efficient Water Treatment Method for Various Sewage: A Review,” *Water Science & Technology*, Vol. 86, No. 2, 2022, pp. 302–320.
- Soyama, H., and Hoshino, J., “Enhancing the Aggressive Intensity of Hydrodynamic Cavitation Through a Venturi Tube by Increasing the Pressure in the Region Where the Bubbles Collapse,” *Aip Advances*, Vol. 6, No. 4, 2016, p. 045113.
- Sullivan, M., “Addressing Perfluorooctane Sulfonate (PFOS) and Perfluorooctanoic Acid (PFOA),” EPA PFAS Summit, May 2018. https://www.epa.gov/sites/production/files/2018-05/documents/dod_presentation_epa_summit_pfos_pfoa_may2018_final.pptx_x.pdf.
- Suryawanshi, P. G., Bhandari, V. M., Sorokhaibam, L. G., Ruparelia, J. P. and Ranade, V. V., “Solvent Degradation Studies Using Hydrodynamic Cavitation,” *Environmental Progress & Sustainable Energy*, Vol. 37, No. 1, 2018, pp. 295-304.
- Tao, Y., Cai, J., Huai, X., Liu, B. and Guo, Z., “Application of Hydrodynamic Cavitation to Wastewater Treatment,” *Chemical Engineering & Technology*, Vol. 39, No. 8, 2016, pp. 1363–1376.
- Thanekar, P. and Gogate, P., “Application of Hydrodynamic Cavitation Reactors for Treatment of Wastewater Containing Organic Pollutants: Intensification Using Hybrid Approaches,” *Fluids*, Vol. 3, No. 4, 2018, p. 98.
- Trang, B., Li, Y., Xue, X.-S., Ateia, M., Houk, K. N. and Dichtel, W. R., “Low-Temperature Mineralization of Perfluorocarboxylic Acids,” *Science*, Vol. 377, 2022, pp. 839–845.
- Vecitis, C. D., Park, H., Cheng, J., Mader, B. T. and Hoffmann, M. R., “Kinetics and Mechanism of the Sonolytic Conversion of the Aqueous Perfluorinated Surfactants, Perfluorooctanoate (PFOA), and Perfluorooctane Sulfonate (PFOS) into Inorganic Products,” *J. Phys. Chem. A*, Vol. 112, No. 18, 2008, pp. 4261–4270.
- Vecitis, C. D., Park, H., Cheng, J., Mader, B. T. and Hoffmann, M. R., “Treatment Technologies for Aqueous Perfluorooctanesulfonate (PFOS) and Perfluorooctanoate (PFOA).” *Frontiers of Environmental Science & Engineering in China*, Vol. 3, No.2, 2009, pp. 129–151.

- Wu, P., Bai, L., Lin, W. and Wang, X., “Mechanism and Dynamics of Hydrodynamic-Acoustic Cavitation (HAC),” *Ultrasonics Sonochemistry*, Vol. 49, 2018, pp. 89–96.
- Zhang, X., Yong, F. U., Zhiyi, L. I. and Zongchang, Z. H., “The Collapse Intensity of Cavities and the Concentration of Free Hydroxyl Radical Released in Cavitation Flow,” *Chinese Journal of Chemical Engineering*, Vol. 16, No. 4, 2008, pp. 547–551.

8 APPENDICES

APPENDIX A: ADDITIONAL DATA

Table 6. Calibration Data Collected During PFAS Analysis CCC = Continued Calibration Check ICV = Initial Calibration Validation (from a secondary source)				
Test	Sample ID	Expected Conc. (µg/L)	Conc. (µg/L)	% Recovery
1. PFOS at 20°C	CCC 1	0.1484	0.1738	117
	CCC 2	0.5938	0.657	111
	ICV 1	0.1484	0.131	88
	SPE Spike 1	0.1	0.1119	112
	SPE Spike 2	0.5	0.4965	99
2. PFOS with H ₂ O ₂	CCC 1	0.0371	0.0419	113
	CCC 2	0.1484	0.1375	93
	CCC 3	0.5938	0.5116	86
	ICV 1	0.1484	0.1275	86
	ICV 2	0.5938	0.5409	91
3. PFOS at pH 4	CCC 1	0.0371	0.0448	121
	CCC 2	0.1484	0.1401	94
	ICV 1	0.1484	0.124	84
	ICV 2	0.5938	0.5764	97
4. PFOS at 40°C	CCC 1	0.0742	0.0797	107
	CCC 2	0.2969	0.2604	88
	ICV 1	0.5938	0.5373	90
5. PFOS 24 hr exp't	CCC 1	0.0371	0.0337	91
	CCC 2	0.2969	0.2614	88
	ICV 1	0.2969	0.2871	97

Table 7. Shorter-Chain PFAS Byproduct

All units in µg/L (ppb)

*branched present but not quantitated due to not having a branched standard

1. Qualifier ratio out of tolerable limits concentration estimated (considered <LOQ)

2. Values estimated due to being at LOQ

PFAS	1: PFOS at 20°C	2: PFOS with H2O2	3: PFOS at pH 4	4: PFOS at 40°C	5: PFOS 24 hr exp't	LOQ	LOD
PFBA	2.50	3.18	2.82	2.98	6.88	1.14	0.346
PFPeA* ¹	2.48	3.11	2.72	2.56	6.13	4.57	1.39
PFHxA*	1.66	2.36	2.27	2.23	4.81	0.286	0.087
PFHpA*	1.12	1.63	1.77	1.57	3.14	0.286	0.087
PFOA*	3.93	4.83	7.46	5.03	5.53	1.14	0.346
PFNA	<LOQ	<LOQ	<LOQ	<LOQ	0.298	0.286	0.087
PFBS ²	0.243	0.234	0.38	0.21	0.334	0.254	0.077
PFPeS*	1.18	1.28	2.75	1.87	1.57	0.269	0.081
PFHxS	7.70	7.45	18.85	10.29	7.61	0.260	0.079
PFHpS*	1.14	1.17	3.99	1.46	0.696	0.271	0.082

APPENDIX B: ANALYTICAL CONFIRMATION WHITE PAPER**THERMAL DESTRUCTION OF PFAS BY HYDRODYNAMIC CAVITATION**

Contract No. W912HQ-22-P-0004

Analytical Confirmation White Paper**July 19, 2022****1 INTRODUCTION**

The Engineering Research and Development Center (ERDC) submitted triplicate matrix matched spiked samples to Eurofins in Lancaster, PA, for analysis of the full sweep of 40 PFAS analytes in Environmental Protection Agency (EPA) Draft Method 1633. Matrix matched samples were spiked and separated into 500 mL bottles to be analyzed by both Eurofins and the ERDC. Samples were submitted for analytical confirmation required for PFAS-related research within the Strategic Environmental Research and Development Program (SERDP). For analytical confirmation, samples must be analyzed by a Department of Defense (DoD) Environmental Laboratory Accreditation Program (ELAP) accredited laboratory. Eurofins (A2LA Cert No. 0001.01), and the ERDC analyzed samples following the Quality Systems Manual (QSM) 5.4, Table B-15. Results of the analysis are summarized in Table 8 and Table 9, and specific sections of the Eurofins data report are attached; the full data package can be provided upon request.

2 ERDC SAMPLE PREPARATION AND ANALYSIS

Samples were prepared using two different methods, solid phase extraction (SPE) and dilution, at the ERDC for comparison to the ELAP-certified laboratory results. SPE samples were collected in 500 mL HDPE bottles with a total volume of 500 mL for analysis, and samples for dilution were collected in 15 mL polypropylene centrifuge tubes with a total volume of 2 mL. Dilution was tested as an alternative sample preparation method in addition to SPE to have an alternative option for highly concentrated samples and those with limited sample volume. For dilution, an equal volume of methanol was added to each sample. Then internal standard was added before going through a 0.2 μ m nylon syringe filter for analysis. The SPE method outlined in EPA Draft Method 1633 was followed for sample extraction and preparation. Samples for analysis contained a final Extracted Internal Standard (EIS) concentration ranging from 1000 to 20000 ng/L for analysis.

All samples were analyzed using liquid chromatography tandem mass spectrometry (LC-MS/MS) using an Agilent 6495C triple quadrupole with jet stream electrospray ionization (ESI) source coupled with a 1290 Infinity II liquid chromatography (LC) system. All samples were analyzed in triplicate using negative mode ESI in dynamic multiple reaction monitoring mode. Two transitions, one as a quantifier and one as a qualifier, were used for quantitation and identification. Quality control samples as outlined in Table B-15 of QSM 5.4 were also analyzed.

Chromatographic separation was performed on a C18 analytical column (Agilent Eclipse Plus RRHD C18 1.8 μ m 2.1x100 mm) coupled with a guard column (Agilent Eclipse Plus C18 2.1 x 5 mm 1.8 μ m) with an Agilent ultrahigh-pressure liquid chromatography system. A delay column (Agilent InfinityLab PFC Delay Column 4.6x30 mm) was installed between the

pump and the autosampler to minimize background contamination potentially coming from solvents, associated tubing, and the pump itself. The analytical column was maintained at 40°C throughout the analysis. The aqueous phase consisted of 2 mM ammonium acetate solution with 3% acetonitrile in LC-MS grade water (A), and 100% LC-MS grade acetonitrile (B). 5 μ L of sample was injected for analysis and the mobile phase flow rate and gradient ratios followed those outlined in EPA Draft Method 1633.

3 ANALYTICAL CONFIRMATION RESULTS

The ERDC and Eurofins both detected all 40 analytes in all three samples. Concentrations for each sample, averages, and percent relative standard deviation (RSD) for each lab and overall percent difference between labs can be found in Table 8 for SPE sample preparation and in Table 9 for dilution. Summary of EIS recoveries can be found in Table 10 for the ERDC and are in the attached report for the ELAP-certified lab. EIS recoveries were between 50% and 150% for all labeled standards except for MPFBA. Method blanks analyzed by ERDC and the ELAP-certified lab were non-detects for all analytes.

4 DISCUSSION

Requirements outlined by the SERDP program specify that ERDC's results preferably need to be within $\pm 30\%$ of the DoD-ELAP accredited laboratory results. For most analytes, ERDC's results fall well within the required criteria, including those that are the focus of this research project, PFOA, PFOS, PFHxS, and their known degradation products. Percent differences between ERDC and Eurofins can be found in Table 8 and Table 9. A second set of triplicate samples (set B) were sent to Eurofins; however, those results are not presented here due to one of the three samples returning with the majority of analytes under limits of quantitation from Eurofins and not having results in triplicate to compare. However, the results for PFBA from set B have been included due to low recovery (below 50%) of MPFBA in the method blank causing bias in set A. The samples in set A needed to be diluted to fit within the linear range for PFAS, and set B was analyzed without dilution. With the dilution of set A, additional labeled standards for quantitation needed to be added to account for the dilution and the low recovery of MPFBA skewed the quantitation of these samples. This shows low recovery of PFBA that is corrected using the isotopic dilution method and is not accounted for in set A due to the additional dilution. The percent difference between labs for PFBA was acceptable in the diluted samples, making it likely that the discrepancies are due to the recovery of PFBA during SPE and not the analytical method itself and will be re-addressed during the quarterly sample comparison. The other analyte that was slightly outside of the suggested $\pm 30\%$ is 6:2 FTS which had a 33% difference between the laboratories. The ELAP-certified laboratory reported the isotopically labeled standard, M2-6:2 FTS as being biased high, which could account for some of this discrepancy. ERDC experienced low recoveries for 3:3 FTCA and PFMPA and therefore those analytes will be removed from the targeted list for now. They will be re-added in the future dependent upon the results of the quarterly comparison with a DoD ELAP certified laboratory. An updated analyte list has been attached to the end of this paper to reflect this change.

The analytes included for the dilution samples were condensed to include the analytes being used in these experiments and their known degradation products since the focus of this study is PFOA, PFOS, and PFHxS. SPE will be the sample preparation method used whenever applicable. When comparing the dilution preparation with the results from the ELAP-certified lab

four analytes were above the ideal 30% that is suggested by SERDP but below 45%. Those analytes were FOSA, 4:2 FTS, 8:2 FTS, and lICI-PF3OUdS. Most analytes were well within accepted criteria when comparing the dilution method results to those of the ELAP-certified lab.

5 SUMMARY

Results shown here are well within the allowed limits for deviation for DoD ELAP accredited laboratory results except for 3:3 FTCA, PFMPA, 6:2 FTS, and PFBA which have all been addressed in the discussion section above. This work demonstrates ERDC's ability to analyze for 38 PFAS analytes within the accepted criteria for SERDP research using SPE as sample preparation and 29 analytes using dilution to prepare samples. The results summarized from this confirmation study supports the ERDC's ability to provide analytical support for the SERDP project Contract No. W912HQ-22-P-001104 using solid phase extraction and dilution when needed for a smaller sub-set of analytes. The ERDC's capabilities will be tested against a DoD ELAP-certified lab quarterly for the duration of this study.

Table 8. Summary of Analytical Results From ERDC SPE Results and the ELAP-Certified Laboratory (continued on the next page)

Analyte	ERDC Analytical Results								DoD ELAP Certified Analytical Results								Percent Difference
	1 (µg/L)	Flag	2 (µg/L)	Flag	3 (µg/L)	Flag	Average	RSD (%)	1 (µg/L)	Flag	2 (µg/L)	Flag	3 (µg/L)	Flag	Average	RSD (%)	
PFBA*	0.39		0.41		0.48		0.43	9.3	N/A		0.39		0.40		0.40	1.3	7.5
PFPeA	0.81		0.78		0.73		0.77	4.2	0.88		0.86		0.90		0.88	1.9	13
PFHxA	0.46		0.44		0.47		0.45	2.7	0.53		0.53		0.70		0.59	14	25
PFHpA	0.47		0.45		0.47		0.46	2.3	0.48	*1	0.44	*1	0.52	*1	0.48	6.8	3.2
PFOA	0.47		0.44		0.46		0.46	2.5	0.46		0.54		0.41		0.47	11	2.3
PFNA	0.46		0.44		0.46		0.45	2.2	0.5		0.53		0.44		0.49	7.6	7.5
PFDA	0.45		0.45		0.47		0.46	1.9	0.51		0.5		0.42		0.48	8.4	4.4
PFUnA	0.49		0.48		0.48		0.48	0.57	0.5		0.56		0.54		0.53	4.7	10
PFDaA	0.47		0.46		0.46		0.46	0.64	0.53		0.51		0.48		0.51	4.1	8.9
PFTTrDA	0.44		0.44		0.44		0.44	0.43	0.39		0.4		0.43		0.41	4.2	8.3
PFTeDA	0.41		0.43		0.41		0.42	2	0.37		0.35		0.38		0.37	3.4	13
FOSA	0.48		0.51		0.48		0.49	2.6	0.5		0.46		0.48		0.48	3.4	1.4
N-MeFOSAA	0.46	M	0.46	M	0.46	M	0.46	0.42	0.51		0.47		0.6		0.53	10	14
N-EtFOSAA	0.48	M	0.47	M	0.48	M	0.48	1.2	0.45		0.56		0.53		0.51	9	7.7
PFBS	0.41		0.41		0.42		0.42	0.97	0.52		0.38		0.5		0.47	13	11
PFPeS	0.46		0.43		0.45		0.45	2.7	0.54		0.5		0.44		0.49	8.3	9.8
PFHxS	0.43	M	0.4	M	0.43	M	0.42	3	0.46		0.46	M	0.45		0.46	1	8
PFHpS	0.53		0.43		0.46		0.47	9.6	0.47		0.49		0.5		0.49	2.6	3
PFOS	0.53	M	0.41	M	0.44	M	0.46	11	0.46		0.48		0.5		0.48	3.4	4.2
PFNS	0.56		0.44		0.47		0.49	10	0.49		0.52		0.46		0.49	5	0.40
PFDS	0.53		0.43		0.44		0.47	10	0.49		0.47		0.43		0.46	5.4	0.40
PFDoS	0.51		0.42		0.43		0.45	8.9	0.33		0.33		0.34		0.33	1.4	30
4:2 FTS	1.7		1.7		1.8		1.7	2.1	1.6	*1	1.3	*1	1.6	*1	1.6	13	9.2
6:2 FTS	1.7		1.7		1.8		1.7	1.8	3.7		2.2		1.3		2.4	41	33
8:2 FTS	1.9		1.7		1.8		1.8	3.8	1.3		1.9		1.6		1.6	15	11

Analyte	ERDC Analytical Results								DoD ELAP Certified Analytical Results								Percent Difference
	1 (µg/L)	Flag	2 (µg/L)	Flag	3 (µg/L)	Flag	Average	RSD (%)	1 (µg/L)	Flag	2 (µg/L)	Flag	3 (µg/L)	Flag	Average	RSD (%)	
3:3 FTCA	0.75		0.72		0.67		0.71	4.9	2.1		1.8		1.9		1.9	6.5	92
5:3 FTCA	8.5		8		8.6		8.4	3.1	9.8		11		11		11	5.3	24
7:3 FTCA	8.4		8		8.4		8.3	2.4	9.9		10		12		11	9.1	25
PFMPA	0.3		0.3		0.25		0.28	8.1	0.69		0.66		0.65		0.67	2.5	82
PFMBA	0.63		0.6		0.58		0.61	3	0.72		0.71		0.74		0.72	1.7	18
NFDHA	0.76		0.73		0.79		0.76	3.4	0.65		0.69		0.68		0.67	2.5	12
PEESA	0.63		0.59		0.63		0.62	2.9	0.57		0.76		0.66		0.66	12	7.6
HFPO-DA	0.69		0.65		0.67		0.67	2.4	0.75		0.8		0.72		0.76	4.4	13
NaDONA	0.58		0.57		0.59		0.58	1.5	0.73		0.84		0.7		0.76	8	26
9CI-PF3ONS	0.63		0.61		0.63		0.62	1.1	0.68		0.76		0.6		0.68	9.6	8.7
11CI-PF3OUdS	0.65		0.64		0.63		0.64	1.4	0.68		0.78		0.63		0.7	9	8.4
N-MeFOSA	0.43		0.44		0.4		0.42	3.5	0.38		0.34		0.34		0.35	5.3	18
N-EtFOSA	0.41		0.42		0.39		0.41	3.6	0.37		0.29		0.32		0.33	10	22
N-MeFOSE	4.2		4.2		4		4.1	1.6	3.9		3.4		3.5		3.6	6	14
N-EtFOSE	4.3		4.2		4.2		4.2	1.1	3.6		3.3		3.4		3.4	3.6	21

Notes: Not applicable (N/A) because sample results were below LOQ; text shown in red represent sample results that are expanded upon in the discussion section; * denotes analytes that sample results were taken from a separate set of samples due to an issue with one of the lab's analyses.

Data Flags: Peak was manually integrated (M); LCS/LCSD RPD exceeds control limits (*1).

Table 9. Summary of Analytical Results for a Subset of Analytes From the ERDC Diluted Sample Results and the ELAP-Certified Laboratory

Analyte	ERDC Analytical Results								Eurofins Analytical Results								Percent Difference
	1 (µg/L)	Flag	2 (µg/L)	Flag	3 (µg/L)	Flag	Avg.	RSD (%)	1 (µg/L)	Flag	2 (µg/L)	Flag	3 (µg/L)	Flag	Avg.	RSD (%)	
PFBA	2.0		2.0		2.0		2.0	0.54	2.2		2.0		2.1		2.1	3.9	5.1
PFPeA	0.97		0.98		0.98		0.98	0.40	0.88		0.86		0.90		0.88	1.9	10
PFHxA	0.49		0.49		0.51		0.50	1.8	0.53		0.53		0.70		0.59	14	16
PFHpA	0.47		0.49		0.50		0.49	2.2	0.48	*1	0.44	*1	0.52	*1	0.48	6.8	1.8
PFOA	0.49		0.49		0.49		0.49	0.34	0.46		0.54		0.41		0.47	11	4.7
PFNA	0.47		0.47		0.49		0.48	2.2	0.50		0.53		0.44		0.49	7.6	3.3
PFDA	0.49		0.47		0.49		0.48	2.1	0.51		0.50		0.42		0.48	8.4	0.47
PFUnA	0.48		0.48		0.46		0.47	2.1	0.50		0.56		0.54		0.53	4.7	12
FOSA	0.30		0.33		0.30		0.31	4.5	0.50		0.46		0.48		0.48	3.4	43
N-MeFOSAA	0.40	M	0.44	M	0.40	M	0.41	4.4	0.51		0.47		0.60		0.53	10	24
N-EtFOSAA	0.39	M	0.40	M	0.39	M	0.39	1.2	0.45		0.56		0.53		0.51	9.0	27
PFBS	0.40		0.44		0.43		0.42	3.5	0.52		0.38		0.50		0.47	13	10
PFPeS	0.47		0.48		0.47		0.47	1.1	0.54		0.50		0.44		0.49	8.3	4.1
PFHxS	0.46	M	0.46	M	0.46	M	0.46	0.27	0.46		0.46	M	0.45		0.46	1.0	0.29
PFHpS	0.44		0.47		0.45		0.45	2.4	0.47		0.49		0.50		0.49	2.6	6.9
PFOS	0.43	M	0.47	M	0.45	M	0.45	3.0	0.46		0.48		0.50		0.48	3.4	7.1
PFNS	0.44		0.47		0.43		0.45	3.8	0.49		0.52		0.46		0.49	5.0	9.9
PFDS	0.37		0.43		0.36		0.39	7.9	0.49		0.47		0.43		0.46	5.4	18
4:2 FTS	2.2		2.3		2.3		2.3	1.1	1.6	*1	1.3	*1	1.6	*1	1.6	13	37
6:2 FTS	2.2		2.3		2.3		2.3	2.0	3.7		2.2		1.3		2.4	41	5.4
8:2 FTS	2.2		2.2		2.3		2.2	1.9	1.3		1.9		1.6		1.6	15	34
PFMPA	0.68		0.68		0.68		0.68	0.32	0.69		0.66		0.65		0.67	2.5	2.3
PFMBA	0.68		0.68		0.69		0.68	0.91	0.72		0.71		0.74		0.72	1.7	5.9
NFDHA	0.77		0.79		0.87		0.81	5.3	0.65		0.69		0.68		0.67	2.5	18
PEESA	0.66		0.64		0.67		0.65	2.1	0.57		0.76		0.66		0.66	12	1.2
HFPO-DA	0.72		0.72		0.73		0.72	0.80	0.75		0.80		0.72		0.76	4.4	4.3
NaDONA	0.61		0.60		0.61		0.61	0.45	0.73		0.84		0.70		0.76	8.0	22
9CI-PF3ONS	0.62		0.62		0.63		0.62	0.72	0.68		0.76		0.60		0.68	9.6	8.6
11CI-PF3OUdS	0.48		0.54		0.51		0.51	5.1	0.68		0.78		0.63		0.70	9.0	31

Table 10. Summary of EIS Recovery by the ERDC				
Standard	Sample 1 (%)	Sample 2 (%)	Sample 3 (%)	Method Blank (%)
MPFBA*	23	23	19	40
M5PFPeA	91	86	88	87
M2 4:2 FTS	92	87	88	82
M5PFHxA	94	91	89	88
M3PFBS	95	88	91	89
M3HFPO-DA	95	89	92	88
1M4PFHpA	89	86	87	87
M3PFHxS	92	90	90	89
M2 6:2 FTS	95	90	92	85
M8PFOA	90	88	88	87
M9PFNA	91	87	87	86
M2 8:2 FTS	94	95	91	81
M8PFOS	81	93	91	84
M6PFDA	94	89	89	90
d3-NMeFOSAA	95	90	92	88
d5-NEtFOSAA	92	89	88	84
M7PFUdA	91	87	86	86
MPFDoA	87	83	84	85
M2PFTeDA	98	92	91	85
M8FOSA	96	88	89	87
d7-NMeFOSE	85	81	81	76
d-NMeFOSA	87	91	90	81
d9-NEtFOSE	82	79	78	78
d-NEtFOSA	96	91	92	79

Updated Analyte List		
Analyte Name	Acronym	CAS Number
Perfluorobutanoic acid	PFBA	375-22-4
Perfluoropentanoic acid	PFPeA	2706-90-3
Perfluorohexanoic acid	PFHxA	307-24-4
Perfluoroheptanoic acid	PFHpA	375-85-9
Perfluorooctanoic acid	PFOA	335-67-1
Perfluorononanoic acid	PFNA	375-95-1
Perfluorodecanoic acid	PFDA	335-76-2
Perfluoroundecanoic acid	PFUnA	2058-94-8
Perfluorododecanoic acid	PFDoA	307-55-1
Perfluorotridecanoic acid	PFTTrDA	72629-94-8
Perfluorotetradecanoic acid	PFTeDA	376-06-7
Perfluorobutanesulfonic acid	PFBS	375-73-5
Perfluoropentanesulfonic acid	PFPeS	2706-91-4
Perfluorohexanesulfonic acid	PFHxS	355-46-4
Perfluoroheptanesulfonic acid	PFHpS	375-92-8
Perfluorooctanesulfonic acid	PFOS	1763-23-1
Perfluorononanesulfonic acid	PFNS	68259-12-1
Perfluorodecanesulfonic acid	PFDS	335-77-3
Perfluorododecanesulfonic acid	PFDoS	79780-39-5
1H,1H,2H,2H-Perfluorohexane sulfonic acid	4:2 FTS	757124-72-4
1H,1H,2H,2H-Perfluorooctane sulfonic acid	6:2 FTS	27619-97-2
1H,1H,2H,2H-Perfluorodecane sulfonic acid	8:2 FTS	39108-34-4
Perfluorooctanesulfonamide	PFOSA	754-91-6
N-methyl perfluorooctanesulfonamide	NMFOSA	31506-32-8
N-ethyl perfluorooctanesulfonamide	NEtFOSA	4151-50-2
N-methyl perfluorooctanesulfonamidoacetic acid	NMeFOSAA	2355-31-9
N-ethyl perfluorooctanesulfonamidoacetic acid	NEtFOSAA	2991-50-6
N-methyl perfluoroactanesulfonamidoethanol	NMeFOSE	24448-09-7
N-ethyl perfluoroactanesulfonamidoethanol	NEtFOSE	1691-99-2
Hexafluoropropylene oxide dimer acid	HFPO-DA	13252-13-6
4,8-Dioxa-3H-perfluorononanoic acid	ADONA	919005-14-4
Perfluoro-4-methoxybutanoic acid	PFMBA	863090-89-5
Nonafluoro-3,6-dioxaheptanoic acid	NFDHA	151772-58-6
9-Chlorohexadecafluoro-3-oxanonane-1-sulfonic acid	9Cl-PF3ONS	756426-58-1
11-Chloroeicosafluoro-3-oxaundecane-1-sulfonic acid	11Cl-PF3OUdS	763051-92-9
Perfluoro(2-ethoxyethane)sulfonic acid	PFEESA	113507-82-7
2H,2H,3H,3H-Perfluorooctanoic acid	5:3 FTCA	914637-49-3
3-Perfluoroheptyl propanoic acid	7:3 FTCA	812-70-4

APPENDIX C: STANDARD OPERATING PROCEDURES

THERMAL DESTRUCTION OF PFAS BY HYDRODYNAMIC CAVITATION

Contract No. W912HQ-22-P-0004

Standard Operating Procedures for PFAS Experiments

1 INTRODUCTION

This SOP details standard operating procedures for collection, preparation, and analysis of PFAS samples for the above-referenced SERDP Limited Scope project, titled “Thermal Destruction of PFAS by Hydrodynamic Cavitation.”

2 SAMPLE COLLECTION

2.1 OVERVIEW

Samples for this project are collected from a 600 mL hydrodynamic cavitation (HC) reactor test loop built at Creare in Hanover, NH. Creare engineers and technicians will mix PFAS-containing aqueous samples of known concentrations, fill the reactor test loop with this solution, operate the reactor to degrade PFAS, and collect samples at defined time points. They will then package these samples and ship them to the ERDC Environmental Laboratory (ERDC-EL) in Vicksburg, MS, for analysis.

2.2 MEDIA AND ANALYTES

2.2.1 PFOS (Perfluorooctanesulfonate)

PFOS was purchased in the potassium salt form from Matrix Scientific (CAS Number 2795-39-3, quantity 5 g). This chemical initially purchased for an EPA SBIR project in August 2020 and has been continuously stored in a chemical cabinet in a temperature-controlled chemistry laboratory. The hazard statements associated with PFOS are given in Table 11.

2.2.2 PFOA (Perfluorooctanoic acid)

PFOA will be purchased from Sigma Aldrich (CAS Number 335-67-1, quantity 100 mg). The hazard statements associated with PFOA are given in Table 11.

2.2.3 PFHxS (Perfluorohexanesulfonate)

PFHxS will be purchased in the potassium salt form from Matrix Scientific (CAS Number 3871-99-6, quantity 1 g). The hazard statements associated with PFHxS are given in Table 11.

Table 11. Hazard Statements Associated With PFAS Chemicals

Hazard Statement	PFOS	PFOA	PFHxS
H301 Toxic if swallowed	X		
H302 Harmful if swallowed		X	X
H314 Causes severe skin burns and eye damage		X	
H315 Causes skin irritation	X		

Table 11. Hazard Statements Associated With PFAS Chemicals			
H317 May cause an allergic skin reaction		X	X
H318 Causes serious eye damage		X	
H319 Causes serious eye irritation	X	X	X
H332 Harmful if inhaled	X	X	X
H335 May cause respiratory irritation	X		
H351 Suspected of causing cancer	X	X	X
H360 May damage fertility or the unborn child	X	X	X
H362 May cause harm to breastfed children	X	X	X
H372 Causes damage to organs through prolonged or repeated exposure	X	X	X
H411 Toxic to aquatic life with long lasting effects	X		X

2.2.4 Diluted Solutions

A dilute solution of 500 µg/L of a single PFAS chemical (PFOS, PFOA, or PFHxS) in distilled water (Poland Springs one gallon bottled distilled water) will be made.

2.2.5 Time Point Samples

We will fill the HC reactor with the dilute solution, degas at conditions that do not produce cavitation, and take 2 mL samples at desired intervals during the experiment, including a sample at time zero prior to any conditions expected to destroy PFAS. The intervals will be selected based on the anticipated approximate destruction rate to ensure adequate capture of the destruction rate dynamics. Between four and ten samples will be taken for each experiment.

2.3 EQUIPMENT/SUPPLIES

2.3.1 Hydrodynamic Cavitation Reactor

Creare built the hydrodynamic cavitation reactor under an EPA SBIR project in 2020. Most of the construction is stainless steel, and care was taken to avoid any components that include fluorocarbon-containing materials, with special attention paid to sealants. The total circulating volume of the reactor is 600 mL.

2.3.2 High-Precision GR-202 Balance

Use a high-precision balance that can accurately measure to 0.00001 g to measure out PFAS chemicals to create dilute solutions.

2.3.3 Polystyrene Weigh Boats, 1.5 Inches Square

Use small polystyrene weigh boats to measure out PFAS chemicals. Pre-crease the weigh boats to aid in material transfer.

2.3.4 Polypropylene Disposable Spatulas, 3.5 mm Diameter

Use a small disposable polypropylene spatula to measure out PFAS chemicals.

2.3.5 1 L Glass Volumetric Flask

Measure out 1 L distilled water in a glass volumetric flask.

2.3.6 1.5 L HDPE Bottle

Dissolve the desired PFAS chemical with distilled water in a 1.5 L HDPE bottle with a polypropylene lid and swirl to mix.

2.3.7 Polypropylene Funnel

Use a polypropylene funnel as needed to transfer liquids to or from the HDPE bottle.

2.3.8 15 mL Polypropylene Centrifuge Tubes

Collect samples in small 15 mL polypropylene centrifuge tubes. Ensure there is not a fluorocarbon seal.

2.3.9 Packaging for Shipment

Samples will be shipped on ice in a small cooler.

2.4 COLLECTION PROCESS

Turn off pump in HC reactor and bring it back to atmospheric pressure. Open the valve to the inlet tank. Open the sample collection valve. Collect the first 5 mL and discard as hazardous waste. Collect the next 2 mL in the sample container (15 mL centrifuge tube) for analysis. Close the sample collection valve and the valve to the inlet tank.

Note that 7 mL of solution will enter the system from the inlet tank when collecting each sample. This is less than 2% of the total reactor volume and will be accounted for in analyzing PFAS breakdown rates.

2.5 DECONTAMINATION PROCEDURES

Triple rinse all containers that come into contact with PFAS chemicals and collect the rinsate as hazardous waste. Then wash with Alconox or Liquinox detergent.

2.6 BOTTLE TYPE

PFAS-containing solutions may be stored in HDPE or polypropylene bottles with HDPE or polypropylene caps.

2.7 FIELD QC TYPES, FREQUENCY, AND CRITERIA

2.7.1 PFAS Contamination in HC Reactor

To test for PFAS contamination in the distilled water source and in the HC reactor, fill the system with distilled water and operate for two hours at conditions expected to destroy PFAS chemicals. Collect a 500 mL sample for analysis.

Perform this QC once before testing with PFAS chemicals. It is considered successful if PFAS contamination is less than 0.1% of the starting PFAS concentration in experiments of 500 µg/L (contamination less than 500 ng/L).

2.7.2 PFAS Destruction Without Hydrodynamic Cavitation

To confirm that conditions used for system filling and degassing do not destroy PFAS chemicals, fill the HC reactor with 500 µg/L PFOS in distilled water and degas. Collect three 2 mL starting point samples. Then operate the reactor at the degassing conditions for two hours. Collect three 2 mL end point samples.

Perform this QC once before conducting experiments to destroy PFAS chemicals. It is considered successful if the average start and end point PFOS concentrations do not exceed $\pm 30\%$ difference.

2.7.3 Duplicate Samples at End Time Point

Collect a 10 mL sample at the end time point so that duplicate PFAS analysis may be done.

2.7.4 Fluorine Mass Balance

For at least one experiment, collect a 2 mL sample and an additional 5 mL sample at the last time point for fluoride ion analysis to complete a fluorine mass balance.

2.8 SAMPLE PRESERVATION, SHIPPING, AND HOLD TIME REQUIREMENTS

2.8.1 Storing Diluted Solutions

Diluted solutions may be stored refrigerated for up to 24 hours before running an experiment in the HC reactor.

2.8.2 Shipping and Hold Time for Collected Samples

Collected samples must be shipped on ice to the ERDC Environmental Laboratory for analysis so that they arrive within 48 hours of sample collection.

3 SAMPLE PREPARATION

3.1 OVERVIEW

Samples for this project will be prepared for analysis by the ERDC-EL using dilution and syringe filter sample clean up due to limited sample volume and samples concentration and will be concentrated as needed. It is possible to use solid phase extraction (SPE) if dilution is proven to be insufficient.

3.2 MEDIA AND ANALYTES

3.2.1 PFAS (Per- and Polyfluoroalkyl Substance) Analytes

This study will be testing PFOA, PFOS, and PFHxS. Samples will be prepared and analyzed using a method that was developed for the 40 PFAS analytes targeted in EPA Draft Method 1633.

3.2.2 Standard Storage

Standards are stored in MeOH at 4°C.

3.3 EQUIPMENT/SUPPLIES

3.3.1 Vortex Mixer

A single vial vortex mixer is used for homogenization.

3.3.2 Disposable Polypropylene Collection Tubes (15 mL)

Polypropylene centrifuge tubes will be used sample collection and preparation.

3.3.3 Reagents and Standards

UHPLC-MS grade methanol was purchased from Sigma-Aldrich. Label extracted internal standards for quantitation were purchased from Wellington Laboratories Inc.

3.3.4 15 mL Polypropylene Centrifuge Tubes

Pipette and Pipette Tips

Manual pipettes of four different sizes (0.5 –10 µL, 10 – 100 µL, 100 – 1000 µL, and 1 – 10 mL) were purchased from Rainin (UNV BioClean Lite XLS). Pipette tips were also purchased from Rainin.

3.3.5 15 mL Polypropylene Syringes

Polypropylene luer lock syringes are used for sample cleanup.

3.3.6 Nylon Syringe Filters

Captiva nylon membrane (polypropylene housing) 0.2 µm syringe filters purchased from Whatman are used for sample cleanup.

3.4 HOMOGENIZATION AND SUBSAMPLING PROCESS

3.4.1 Homogenization

Samples will be vortexed for 30 s to homogenize and inverted by hand.

3.4.2 Subsampling

Samples will only be subsampled after they have been diluted with MeOH in the original collection vessel to ensure the sample is in 50% organic.

3.5 PREPARATION TECHNIQUES

3.5.1 Dilution

Due to limited sample volume and concentration, dilution will be the preparation technique for analysis. An equal volume of MeOH will be added to the sample in the original sampling vessel. SPE and/or a concentration step will be considered if the dilution method is proven to be insufficient. The SPE procedure outlined in Draft Method 1633 will be implemented if needed.

3.6 CLEANUP PROCEDURES

3.6.1 0.2 µm Nylon Syringe Filter

Samples will go through a 0.2 µm nylon syringe filter after the addition of extracted internal standards and MeOH for sample cleanup.

3.7 SAMPLE PREPARATION QC TYPES, FREQUENCY, AND CRITERIA

3.7.1 Continuing Calibration Verification (CCV)

A CCV is run at the start of each analytical batch analysis, after every 10 samples, and at the end of the sequence. Analyte concentrations must range from limit of quantitation (LOQ) to the concentration of the mid-level calibrator. Analyte recovery must be within 70% to 130% of the true value.

3.7.2 Laboratory Control Sample (LCS)

A blank spiked with all analytes \geq LOQ and \leq the midlevel calibrator concentration will be run once per sample batch.

3.7.3 Matrix Spike (MS) and Matrix Spike Duplicate

A sample spiked with all analytes \geq LOQ and \leq midlevel calibrator and a duplicate will be analyzed with each sample batch.

3.7.4 Post-Spike Sample

Since dilution will be the primary method of sample preparation for this project, any sample that report analytes $<$ LOQ will be spiked and analyzed again. Analytes reported $<$ LOQ will be spiked into the sample and must recovery within 70% to 130%. This will be done specifically for PFOA, PFOS, and PFHxS as they are the analytes that are being tested in this study.

3.8 SAMPLE EXTRACT STORAGE AND HOLDING TIME REQUIREMENTS

3.8.1 Holding Times

Aqueous samples will be stored up to 90 days in -20°C when available. When stored at 0° to 6°C , samples will be analyzed within 28 days in accordance with Draft Method 1633.

4 SAMPLE ANALYSIS

4.1 OVERVIEW

Samples for this project will be quantitated using liquid chromatography triple quadrupole mass spectrometry (LC-QqQ-MS). All criteria for quantitation in QSM 5.4 Table B-15 are followed this analysis.

4.2 MEDIA AND ANALYTES

4.2.1 PFAS (Per- and Polyfluoroalkyl Substance) Analytes

The analytical method used for quantitation follows Draft Method 1633 and targets the 40 analytes listed.

4.3 EQUIPMENT/SUPPLIES

4.3.1 Reagents

UHPLC-MS grade methanol was purchased from Sigma-Aldrich (CAS number: 67-56-1). Optima grade acetonitrile was purchased from Fisher Chemical (CAS number: 75-05-8). LC-MS grade water was purchased from Honeywell (CAS number: 7732-18-5). LC-MS grade isopropyl alcohol was purchased from Supelco LiChrosolv (CAS number: 67-63-0). Ammonium acetate for mass spectrometry was purchased from Sigma Aldrich (CAS number: 631-61-8).

4.3.2 Standards

Native and labeled PFAS analyte mixtures were purchased from Wellington Laboratories to include all natives, EIS, and NIS included in Draft Method 1633. The mixtures purchased are as follows: PFAC-MXF, PFAC-MXG, PFAC-MXH, PFAC-MXI, PFAC-MXJ, MPFAC-HIF-ES, and MPFAC-HIF-IS. A PFAS mixture to act as a secondary source includes 24 PFAS analytes and was purchased from Absolute Standards.

4.3.3 Instrumentation

Ultrahigh-performance liquid chromatograph (Agilent Infinity 1290 II) equipped with tandem quadrupole mass spectrometer (Agilent 6495C TQ). Agilent PFC Delay column (4.6 x 30 mm) is in place between the pump and autosampler to delay potential PFAS inherently in the instrument ensuring that they elute after sample peaks. An Agilent Poroshell 120 EC C18 (1.9 μ m 2.1 x 100 mm) analytical column is used for separation. Both columns are equipped with a guard column (Agilent Eclipse Plus C18, 2.1 x 5 mm 1.8 μ m) to extend column life.

4.3.4 Certified Reference Standards

Certified reference standards in MeOH purchased from Wellington Laboratories will be used for all analytical work.

4.3.5 Branched and Linear

The standard solutions used for this work include branched and linear forms for PFOS, PFH_xS, NEtFOSAA, and NMeFOSAA.

4.4 CALIBRATION PROCEDURE

4.4.1 Isotope Dilution

Labeled standards will be added to samples prior to dilution and sample cleanup. When available, a direct labeled match to natives will be used for quantitation. Direct matches are available for PFOS, PFOA, and PFH_xS. EIS listed in Draft Method 1633 will be used for quantitation.

4.5 INSTRUMENT CLEANLINESS REQUIREMENTS

4.5.1 Instrument Cleanliness Monitoring

Instrument background levels are monitored before and after every sample batch. All sample batches begin with two no inject sample runs with open windows to monitor delay peaks,

followed by a no inject using the normal method to monitor any protentional contamination after the delay column. Lastly, methanol without any standards is also monitored.

4.5.2 Blank Criteria

Instrument blanks are run after the highest standard and prior to sample analysis. Concentrations of all analytes must be below ½ the LOQ. Blank criteria is in agreement with QSM 5.4 Table B-15.

4.6 CALIBRATION VERIFICATION

4.6.1 Initial Calibration Verification

Using a second source standard prior to sample analysis. Analyte concentrations must be within $\pm 30\%$ of their true value.

4.6.2 Instrument Sensitivity Check

Analyzed at LOQ and concentration must be within $\pm 30\%$ of their true value.

4.6.3 CCV

A CCV is run at the start of each analytical batch analysis, after every ten samples, and at the end of the sequence. Analyte concentrations must range from LOQ to the concentration of the mid-level calibrator. Analyte recovery must be within 70% to 130% of the true value.

4.6.4 LCS

A blank spiked with all analytes \geq LOQ and \leq the midlevel calibrator concentration will be run once per sample batch. Analyte recovery must be within 70% to 130% of the true value.

4.6.5 Criteria

Table 12 shows the criteria that will be followed for all quantitative analysis. Values are in accordance with QSM 5.4 Table B-15.

Table 12. Quantitative Analysis Requirements	
QC Element	Criteria
Sample Precision	$\pm 30\%$ RPD
Sampling Bias	Not detected or $< \frac{1}{2}$ LOQ
Sample Preparation Precision	$\pm 30\%$ RPD
Sample Preparation Bias	Analytes must be within 70 - 130% recovery
Detection/Quantitation Limit	S/N > 10 for quantitation ions and > 3 for confirmation ions
	Quantitation ions (PFOA: 413 \rightarrow 369, PFOS: 499 \rightarrow 80, PFHxS: 399 \rightarrow 80)
	Ion ratios cannot exceed 50 – 100%
Calculations	$\text{Concentration (native analytes)} = \frac{\text{Area}_n \times M_1}{\text{Area}_1(\text{RR})} \times \frac{1}{W_s}$ <p> Area_n = Measured area of quantifier ion for the native PFAS Area₁ = Measured area of quantifier ion for the labeled PFAS M₁ = Mass of labeled compound added RR = Average response ratio to quantify target compounds W_s = Sample volume (L) </p>

4.7 KNOWN INTERFERENCES

4.7.1 Instrument Contamination

Instrument background levels of PFAS are monitored before and after every analytical sample batch.

4.7.2 Solvents for Sample Preparation and Analysis

Solvents will be monitored for PFAS contamination, each new lot will be tested before use, and all targeted analytes must be below $\frac{1}{2}$ the LOQ.

4.8 VERIFICATION OF NUMERIC DETECTION/QUANTITATION VALUE

4.8.1 Certified Laboratory Comparison

Quarterly comparison at three concentrations ($n = 3$ for each concentration) with a DoD ELAP accredited lab. The average of the three replicates will be compared and must not exceed $\pm 30\%$ difference.

APPENDIX D: SAFETY MEMORANDUM

CREARE MEMORANDUM

IM-22-04-080

April 14, 2022

TO: CLD, ADuffy, MGIzenson, MDJ (Safety Officer), DKromer, KTM, MXS
(Backup Safety Officer)

CC: JWO, RPK, JKS, DWeinstein, Project Folder, Safety Department Folder

FROM: RGilmore

SUBJECT: SAFETY REVIEW – PFAS CAV (#1010427)

1 INTRODUCTION

For project “PFAS CAV” we plan to *destroy PFAS chemicals in water using hydrodynamic cavitation*. This activity has safety issues regarding the following:

- High-voltage pump (230 V).
- High-pressure fluids (< 175 psi).
- Using water near electrical equipment.
- Hazardous chemicals – methylene blue, perfluorooctanesulfonic acid (PFOS), perfluorooctanoic acid (PFOA), and perfluorohexane sulfonate (PFHxS).

This Safety IM is a revision of IM-20-08-142 associated with PFAS Destroy (#1010292) and PFAS Pilot IRAD (#10IRAND.00.102). The key changes in this revision are as follows:

- Updated process conditions, including recovery pressures of 30 to 90 psia, pump speeds of 14 to 30 Hz, flow rates of 1 to 8 gpm, and the use of additional orifice plates with varying numbers and sizes of the holes. Modified instructions for degassing the test facility to be applicable for this range of conditions.
- The addition of a flow meter and a sight glass for a spectrometer to the test facility in the Centerra fume hood. Modified draining procedure to account for these new elements.
- Conducting experiments with two additional types of per- and polyfluoroalkyl substances (PFAS): PFOA and PFHxS (see Table 1 for hazard summary).
- Mixing solutions in the fume hood at Creare and transporting them to Centerra for use in our test facility.
- Making a concentrated methylene blue stock solution and using it to create the dilute solutions, rather than weighing out methylene blue for each experiment.


IM-22-04-080
April 14, 2022

- Clarifying that methylene blue is not classified as a hazardous material by the State of New Hampshire, but it cannot be poured down the drain. Thus, we must collect liquid waste for disposal, but solid waste can go into the regular trash/landfill.
- Performing more experiments and generating more hazardous waste.

2 GENERAL DESCRIPTION OF THE ACTIVITY OR SAFETY ISSUE

2.1 BACKGROUND

Per- and polyfluoroalkyl substances (PFAS) are used in numerous household and industrial goods, including nonstick and waterproof coatings and firefighting foams. These substances have contaminated ground and drinking water sources and cause long-term adverse health effects. They are called “forever chemicals” because they do not break down naturally in the environment. We propose hydrodynamic cavitation as a novel technology for destruction of PFAS in water.

In hydrodynamic cavitation, a low-pressure region is created by methods such as accelerating water through a Venturi nozzle or orifice plate. As the water velocity increases, the static pressure falls. If the local static pressure falls below the water’s vapor pressure, then bubbles form and grow in the water. When the static pressure level is later recovered, such as when the water exits an orifice plate, the bubbles rapidly collapse, and extremely high local pressure and temperature conditions are produced.

The orifice geometry is characterized by the dimensionless number γ , which is the ratio of the total flow area of the orifice to the cross-sectional area of the pipe. In the case where the orifice plate contains multiple orifices:

$$\gamma = \frac{Nd^2}{D^2}$$

where D is the pipe diameter, d is the diameter of an orifice, and N is the number of orifices in the plate. For an orifice plate with a single orifice in the center of the plate, γ simplifies to d^2/D^2 , which is the square of the familiar dimensionless number $\beta=d/D$ that is used to characterize orifice flow meters. γ values of 0.1 to 0.2 typically give good performance in the HC systems cited in the literature.

Whether or not cavitation will occur is predicted by the dimensionless cavitation number, C_v , which is defined as:

$$C_v = \frac{P_2 - P_v(T)}{0.5\rho(v_2/C_c)^2 - \Delta P_{exp,l}}$$

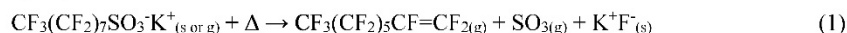
where P_2 is the recovery pressure, P_v is the vapor pressure of the liquid, ρ is the density of the liquid, and v_2 is the velocity at the throat of the constriction. C_c accounts for the fact that the throat diameter of the pumped liquid is smaller than the orifice diameter and is given by $C_c = \frac{A_c}{A_2} = 1 - \frac{1-\gamma}{2.08(1-\gamma)+0.5371}$. $\Delta P_{exp,l}$ is the irreversible pressure drop associated with expansion and is given by


IM-22-04-080
April 14, 2022

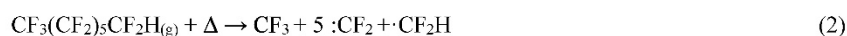
$\Delta P_{exp,I} = (1 - \gamma)^2 0.5 \rho v_2^2$. Cavitation occurs when the cavitation number is equal to or less than one, with lower cavitation numbers generally indicating more intense cavitation.

Hydrodynamic cavitation destroys PFAS chemicals such as PFOS through the following degradation mechanism proposed by Vecitis et al. (2009)¹:

1. Pyrolysis at the bubble interface cleaves the C-S bond:



2. Pyrolysis in the bubble vapor breaks fluorocarbon intermediates into C1 fluororadical constituents:



3. C1 fluororadicals react with H₂O, HO, H, and O-atom in the bubble vapor to yield CO, CO₂, and HF byproducts. HO, H, and O-atom are generated by thermolytic splitting of water in the bubble vapor.

We note that the concentrations of CO, CO₂, and HF generated is limited by the initial concentration of PFOS in the system, which is 500 ppb in this project. If all C-F bonds in PFOS were broken, this would correspond to a fluoride ion concentration of about 0.3 mg/L. For reference, the optimal fluoride ion level in drinking water to prevent tooth decay is 0.7 mg/L.

2.2 EXPERIMENTS WITH WATER

We have built the laboratory-scale experimental setup shown in Figure 1 and Figure 2 to demonstrate hydrodynamic cavitation. Generating intense bubble collapse requires high recovery pressures and flow rates, necessitating the selection of a large pump (Liquiflo Model HF9, <http://www.liquiflo.com/v2/gears/h/h9f.htm>). The total volume of this system is 1000 mL, and we considered the ease of draining and rinsing in our system design.

We conducted initial experiments with water as the working fluid. Conditions tested are shown in Figure 3. We excluded conditions where the pressure relief valve was tripped or where the flow rate and the pressure drop across the orifice had stopped increasing with increasing motor speed. Cavitation occurred at conditions shown with a solid filled circle, and these conditions provide the most promising conditions for experiments with hazardous chemicals. We also practiced filling, draining, and flushing the experimental setup, and we measured the system volume at 1000 mL.

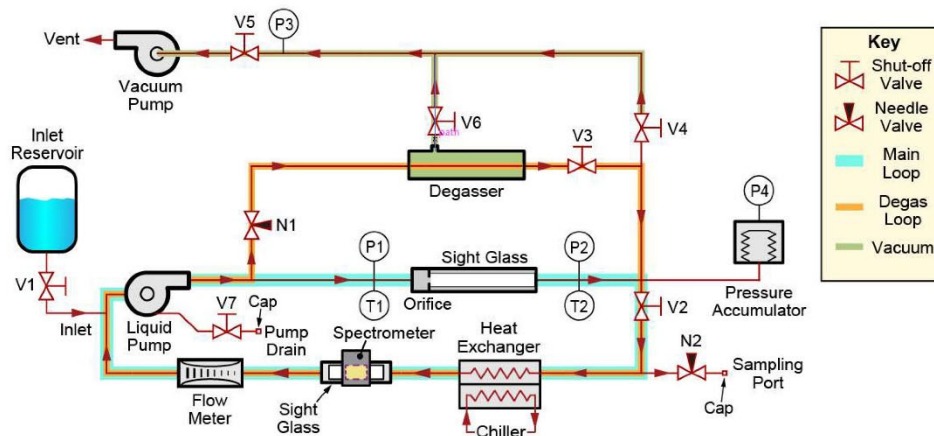
2.3 EXPERIMENTS WITH HAZARDOUS MATERIALS

We plan to run experiments with the hazardous materials below at pump motor speeds of 14 to 28 Hz, and recovery pressures of 30 psia to 90 psia. We will test only at conditions we have

¹ Vecitis, C. D., Park, H., Cheng, J., Mader, B. T. and Hoffman, M. R., "Treatment Technologies for Aqueous Perfluorooctanesulfonate (PFOS) and Perfluorooctanoate (PFOA)," Front. Environ. Sci. Eng. China, Vol. 3, 2009, pp. 129–151.

previously tested with distilled water (Figure 3). Each test is expected to generate a maximum of 12 L (3.2 gal) of hazardous waste.

1. Run experiments with 15 μmol methylene blue in water (5 mg/L). Methylene blue is a hydroxyl scavenger that has been used as an indicator for $\text{HO}\cdot$ generation in hydrodynamic cavitation (Li et al. 2017).² Its bright blue color makes it straightforward to measure the concentration using a simple absorption measurement. Generation of hydroxyl radicals is essential for the breakdown of C1 fluororadicals from PFAS chemicals, so these experiments will allow us to identify the most promising conditions for testing with PFOS. Methylene blue is not classified as hazardous waste by the State of New Hampshire, but it cannot be poured down the drain, so we will be collecting it following hazardous waste collection procedures. We plan to run up to eight experiments with methylene blue.
2. Run experiments with 500 ppb PFOS in water (0.5 mg/L). Send select samples to the ERDC Environmental Lab in Vicksburg, MS, for detailed analysis of breakdown products. RPK has confirmed that there are no restrictions on shipping PFOS in water at this time. We plan to run up to four experiments with PFOS.
3. Run experiments with 500 ppb PFOA or PFHxS in water. Send select samples to the ERDC Environmental Lab in Vicksburg, MS, for detailed analysis of breakdown products. We plan to run one experiment with PFOA and one with PFHxS.



\\OLYMPUS\Projects\1010427-PFAS-CAV\Technical Work\Graphics\Schematics-2022-04-11_PFAS-CAV-1

Figure 1. Bench-Scale Hydrodynamic Cavitation Test Facility Schematic

² Li, X., Huang, B., Chen, T., Liu, Y., Qiu, S., & Zhao, J., "Combined Experimental and Computational Investigation of the Cavitating Flow in an Orifice Plate with Special Emphasis on Surrogate-Based Optimization Method," *Journal of Mechanical Science and Technology*, Vol. 31, No. 1, 2017, pp. 269–279.

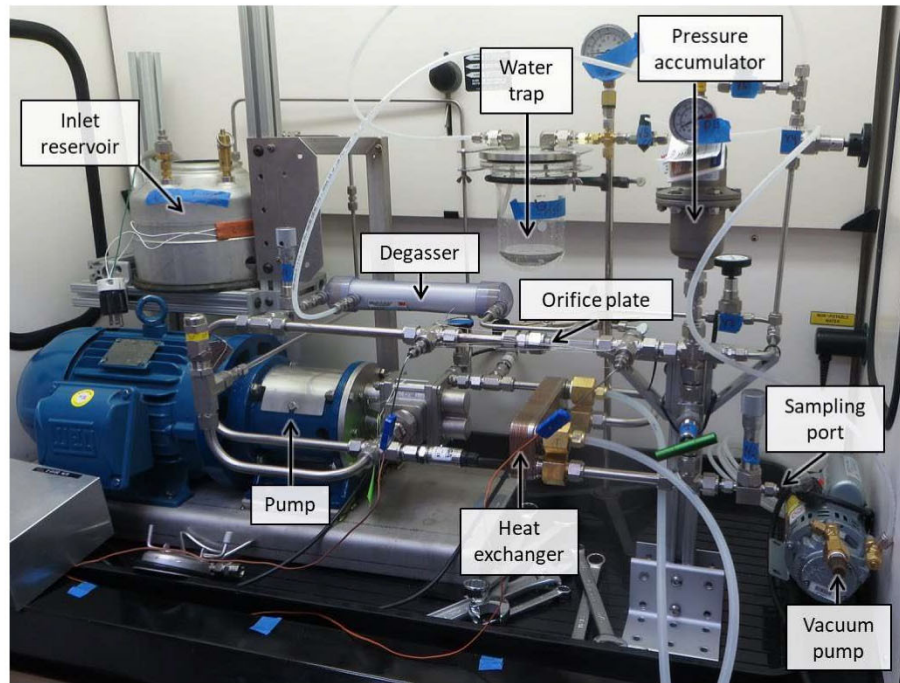


Figure 2. Bench-Scale Hydrodynamic Cavitation Test Facility Photo

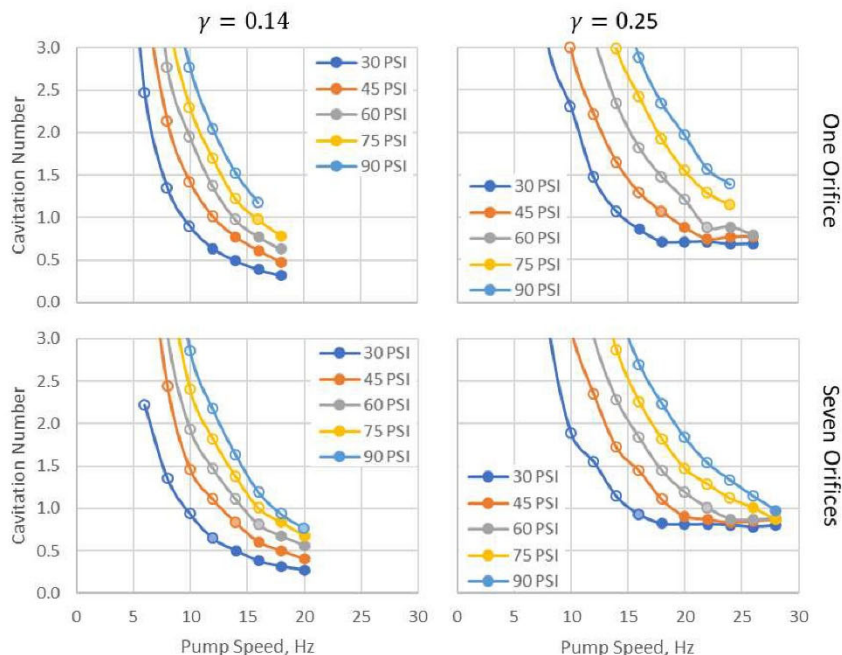


Figure 3. Estimated Cavitation Number for Four Different Orifice Plates as a Function of the Liquiflo Pump Motor Speed and Recovery Pressure (P2) in Water Testing. Open circles indicate no cavitation, shaded circles indicate weak cavitation, and solid circles indicate clear cavitation. Operating conditions that were not stable are omitted.

3 HAZARDS AND MITIGATION STRATEGIES

1. **High-voltage pump (230 V).** The pump (Liquiflo Model HF9 <http://www.liquiflo.com/v2/gears/h/h9f.htm>) and driver (Lenze SMVector VFD ESV222N04TXC Drive NEMA 4X) operate at 230 V. Electrical wiring between the driver and pump was completed by the supplier. A 208 V three-phase power supply was professionally installed with a circuit breaker in the Centerra Chem Lab electrical panel in 2020 for the PFAS Destroy (#1010292) project. Wiring from the wall to the pump was done by a Creare E-lab technician (BMP). An emergency stop button mounted in an enclosure with a 24 V power supply is incorporated between the wall source and the driver. There are no exposed wires or connections, and all components are well grounded. We have posted high voltage signs near the pump.


IM-22-04-080
April 14, 2022

This pump is heavy—about 230 lbs. We have placed it on rubber feet within the containment tray (described below) to distribute load and reduce vibration impact. The stated weight capacity of the cabinets below the fume hood is 500 lbs per linear foot. This fume hood is 5 ft wide, so the expected capacity is 2500 lbs, which includes the weight of the countertop and fume hood above. Since our pump and assorted other equipment is only about 10% of the capacity, we are not concerned that we will approach this weight limit.

The Liquiflo pump is quieter than the vacuum pump, and hearing protection is not required for either. However, some users may find using hearing protection when operating the vacuum pump more comfortable, so it should be available.

2. High-pressure fluids. The positive displacement pump is capable of generating high differential pressures, up to 125 psid with water as the working fluid (the motor may fault and shut off at about 130 psid). In a closed-loop system, as planned here, pressures can be driven even higher. The high-pressure part of the system is between the pump outlet, the orifice, and the needle valve to the degasser (N1). Pressure in the low-pressure part of the system is set by the pressure accumulator to a maximum of 90 psia. We include a pressure relief valve near the pump outlet that is set to 175 psig, which sets the maximum pressure of the system. We note that this maximum pressure was selected for the PFAS Destroy project when the maximum recovery pressure was set to 60 psia; it may be desirable to increase the pressure relief valve to 205 psig if we find that higher recovery pressures would be beneficial for improving PFAS destruction. Because this system will be used with hazardous liquids, this relief valve empties into the inlet tank, which will have an air void fraction at the top and be vented to atmosphere. The lowest rated system component in the high-pressure part of the system is the safety valve itself, which has a rating of 225 psig. We have proof tested the orifice assembly to 375 psia.

In the low-pressure region of the system, the degasser pressure rating is only 116 psig for the liquid side and 87 psig on the gas side. Under expected continuous flow operation, the pressure drop in the degasser bypass line occurs primarily across the needle valve (N1); at 750 mL/min, the expected pressure drop across the needle valve is 100 psi, whereas the expected pressure drop across the degasser is 2 psi, so the degasser is expected to see essentially the same pressure as the pressure accumulator (set to a maximum of 90 psia or 75 psig). However, the degasser bypass line is only used during setup and degassing at a recovery pressure of up to 30 psia and at low enough pump speeds to keep the pressure drop below 70 psia and ideally below 50 psia, so the maximum pressure in this line would be 100 psia (85 psig) and ideally only 80 psia (65 psig).


IM-22-04-080
April 14, 2022

By not following protocols, it may be possible for a user to over pressurize the degasser and cause a leak in the system. If a user were to close V3 but not N1, and then increase the pump speed, it is possible that the degasser could equilibrate with the high-pressure side of the system, see higher pressures, and fail. The expected failure mode in the degasser is that the membrane will break and liquid will leak into the gas side, which empties into a water trap. The water trap is designed to be used with vacuum, and the gasket will unseat above ~3 to 5 psig. If V6 were also closed, the gas side could potentially over pressurize and leak as well. Warnings are included in the directions below to prevent this, as well as additional shielding as described below.

As an added precaution, we use a containment tray in the fume hood under the system (Figure 4). The selected tray is made of polypropylene about 1/8" thick with dimensions of 47 L x 21.5 W x 1.5 H and an internal capacity of 28 L. The tray was selected to fit the fume hood well and maximize the useable footprint for our setup while still providing good airflow, and holding much more than the expected system volume. Additional shielding with a clear plastic curtain or clear polycarbonate sheet is incorporated to direct any fluid spray downward into the tray when testing with hazardous chemicals. Care will be taken to try to keep sufficient air gaps to allow vent flow through the containment zone and to keep the pump motor exposed so it can release heat to the hood flow.

All procedures are tested first with water to ensure operation as expected before using hazardous chemicals.

3. Using water near electrical equipment. We are using a pump to move water and aqueous solutions, which needs to be in the fume hood, in the containment tray. Electrical wires are shielded and protected. No standing water is expected in the setup. In the event of a leak or spill, we will use the E-stop mounted on the left side of the hood to cut power to the pump before cleaning up the spill.
4. Hazardous chemicals.

Hazards: Methylene Blue. Methylene blue was purchased as a crystalline powder (Creare SDS Number 6636, CAS Number 122965-43-9, quantity 25 g) for PFAS Pilot IRAD (#10IRAND.00.102). This chemical has been stored in the Centerra Chem Lab chemicals hood and will be used again on this project. The hazard statement associated with methylene blue is "Acute toxicity, Oral (Category 4), H302: Harmful if swallowed." Additional precautionary statements relate to washing skin after handling, not eating, drinking, or smoking while using, and disposing to an approved waste disposal plant. Methylene blue is not classified as hazardous waste by the State of New Hampshire, but it cannot be poured down the drain. Therefore, we are collecting aqueous solutions of methylene blue following hazardous waste collection procedures. Solids such as rinsed weighing trays, spatulas, Kimwipes, or gloves may go in the regular trash.


IM-22-04-080
April 14, 2022

Hazards: PFOS. Perfluorooctanesulfonate (PFOS) was purchased in the potassium salt form (Creare SDS Number 6639, CAS Number 2795-39-3, quantity 5 g), which is a powder, on PFAS Destroy (#1010292). This chemical has been stored in the Centerra Chem Lab chemicals hood and will be used again on this project. The hazard statements associated with PFOS are given in Table 1. PFOS is an aquatic hazard and should never be poured down the drain. Additional precautionary statements advise avoiding breathing dust, fumes, gas, mist, vapors, or spray; to call a poison center or doctor if swallowed; and to rinse eyes for several minutes if in eyes.

Table 1. Hazard Statements Associated With PFAS Chemicals			
Hazard Statement	PFOS	PFOA	PFHxS
Creare SDS Number	6639	TBD	TBD
H301 Toxic if swallowed	X		
H302 Harmful if swallowed		X	X
H314 Causes severe skin burns and eye damage		X	
H315 Causes skin irritation	X		
H317 May cause an allergic skin reaction		X	X
H318 Causes serious eye damage		X	
H319 Causes serious eye irritation	X	X	X
H332 Harmful if inhaled	X	X	X
H335 May cause respiratory irritation	X		
H351 Suspected of causing cancer	X	X	X
H360 May damage fertility or the unborn child	X	X	X
H362 May cause harm to breastfed children	X	X	X
H372 Causes damage to organs through prolonged or repeated exposure	X	X	X
H411 Toxic to aquatic life with long lasting effects	X		X

Hazards: PFOA. Perfluorooctanoic acid (PFOA) will be purchased from Sigma Aldrich (CAS Number 335-67-1, quantity 100 mg). The hazard statements associated with PFOA are given in Table 1.

Hazards: PFHxS. Perfluorohexanesulfonate (PFHxS) will be purchased in the potassium salt form from Matrix Scientific (CAS Number 3871-99-6, quantity 1 g). The hazard statements associated with PFHxS are given in Table 1.


IM-22-04-080
April 14, 2022

Hazards as Aqueous Solutions. The vapor pressure of PFOS is 0.002 mmHg, of PFOA is 0.52 mmHg, and of PFHxS is 0.0046 mmHg, and the vapor pressure of methylene blue is 7.0×10^{-7} mmHg, whereas the vapor pressure of water is 23.8 mmHg at 25°C. Therefore, the primary hazards of the diluted solution forms of these chemicals are expected to be through direct contact (skin, swallowing, etc.), rather than inhalation or vapor contamination.

Precautions and PPE. Use only in a chemical fume hood. This includes measuring powders and handling diluted solutions. The test facility has been assigned space in a fume hood in the Centerra Chem Lab. Dilute solutions will be made in the Great Hollow Chem Lab. Dilute solutions will be transported from Great Hollow to Centerra in secondary containment (<https://www.mcmaster.com/40015T81/>). Wear appropriate PPE, including splash goggles, nitrile gloves, and a splash apron. Breakthrough time for methylene blue, PFOS, PFOA, and PFHxS is 480 minutes for 0.11 mm thick nitrile gloves (source: Sigma Aldrich MSDS). Use 4 mil (0.11 mm) thick nitrile gloves when working with diluted solutions, and 10 mil thick nitrile gloves when working with raw materials to provide added protection against pinholes.

Purchase Quantities. Purchase minimum available quantities. Reuse the methylene blue (25 g, Sigma-Aldrich, CAS Number 122965-43-9) and PFOS (5 g, Matrix Scientific, CAS Number 2795-39-3) from PFAS Pilot IRAD and PFAS Destroy. To date, minimum quantities are 100 mg PFOA from Sigma Aldrich (CAS Number 335-67-1) and 1 g PFHxS from Matrix Scientific (CAS Number 3871-99-6).

Chemical Storage. Chemicals will be stored in the Great Hollow Chem Lab. Based on the SDS, storage for all is in the combustible storage class, and PFAS are also in the acute toxic Cat. 3 class.

Creating Concentrated Methylene Blue Solution. Create a 15 mmol/L methylene blue stock solution to facilitate repeated methylene blue testing. Measure 0.048 g methylene blue using a disposable weighing tray and a disposable polypropylene spatula in the fume hood. Dissolve the methylene blue in 10 mL distilled water. Triple rinse any containers used to hold the diluted solutions and discard rinsate as hazardous waste. Discard the weighing tray and spatula in the trash. Store the concentrated solution in a clearly labeled HDPE bottle with a tight-fitting lid in secondary containment in a fume hood or flammables cabinet. We do not expect any outgassing from the methylene blue solution.

Creating Diluted Methylene Blue Solution. Use a micropipette to measure 1 mL of the 15 mmol/L methylene blue stock solution into a larger container and dilute to 1 L with distilled water.

Creating Diluted PFAS Solutions. Use disposable weighing tray and polypropylene spatula to measure small quantities (0.5 mg PFOS) using a high precision balance (five decimal places) in a fume hood. Dissolve in (1 L) water in the fume hood. Discard disposable tray and spatula as hazardous waste. Triple rinse any containers used to hold the diluted solutions and discard rinsate as hazardous waste.


IM-22-04-080
April 14, 2022

Waste Quantities. Expected waste quantities for methylene blue are ~18 L (1 L from experiment and 1 L from rinsates for each of up to eight experiments, plus an extra 2 L for additional rinses before switching to PFAS chemicals). Expected waste quantities for PFOS are ~17 L (1 L from experiment and 3 L from rinsates for each of up to four experiments, plus an extra 1 L rinse at the conclusion of PFOS testing). Expected waste quantities for PFOA and PFHxS are ~5 L each (1 L from experiment and 4 L from rinsates for one experiment each). The waste container holds 19 L (five gallons). PFAS chemicals including PFOS, PFOA and PFHxS may be combined into a single waste stream.

Spills. For solids, wipe up dry material and dispose as solid hazardous waste. Then wipe with a damp towel. Then wipe with soapy towel. Dispose of all towels as hazardous waste. For liquids, use paper towels or spill pillows to soak up liquid. Wash area with soap and water. Dispose of all materials as hazardous waste. For a large spill of PFAS (PFOS, PFOA, or PFHxS, liquid or solid) outside the fume hood, ensure lab fume hoods are on and drawing air, leave the lab, and post a sign on the door not to enter. Then contact the Chemical Spill Response Team and the Safety Officer for assistance.

Cleanup. Drain system at low point. Experimental setup should be triple rinsed after methylene blue testing and quadruple rinsed after PFAS testing and all rinsate discarded as hazardous waste. The system volume is 1 L, so expected waste volume is about 4 or 5 L per test if the system is fully rinsed between each test. However, it is not necessary to fully rinse the system between tests with the same material, which will limit the quantity of hazardous rinsates generated. If the system is not fully rinsed, it is considered contaminated, should only be touched with gloves, and must remain in the fume hood.

Chemical Waste Disposal. Hazardous waste generation is expected to occur over a period of a few months for each chemical. An appropriate container should be selected that will hold all liquid waste including rinsate generated from that chemical. These five-gallon jugs from McMaster are a good choice: <https://www.mcmaster.com/4135T23>. Fill these jugs carefully, ensuring no liquid contaminates the outside, then double bag, label, and store in secondary containment below the PFAS CAV bench in the main labs at Centerra. Use separate waste streams for methylene blue and PFAS. Solid materials such as gloves, Kimwipes, paper towels, weighing trays, etc. that may have been contaminated by PFAS chemicals should be collected as solid hazardous waste in a jug or pail (<https://www.mcmaster.com/3995T439/>, <https://www.mcmaster.com/3995T459/>). When a waste container is full or at the conclusion of testing with a particular chemical and/or the project, contact RPK to arrange waste disposal.

4 SPECIFIC PROCEDURES AND PROTOCOLS

Only qualified system operators who have signed this safety IM and had Creare Chem Lab safety training and hazardous waste training may perform the procedures listed in this document.


IM-22-04-080
April 14, 2022

4.1 PROCEDURES FOR MEASURING DILUTED SOLUTIONS

4.1.1 Work Area and Containment Materials

1. All chemical work must be performed in a fume hood by trained personnel. Wear 10 mil nitrile gloves when handling raw materials and creating diluted solutions. Wear 4 mil nitrile gloves when handling diluted solutions. In both cases, wear safety goggles and a splash apron.
2. Have adequate spill pillows, paper towels, and Kimwipes available to be able to clean up a 1 L liquid spill.
3. Verify that the fume hood blower is on and flow velocity is in the range of 60 to 100 ft/minute.
4. Ensure a calibrated 5 decimal (0.00001 g) balance is in the fume hood.
5. Label a 1 L HDPE shipping bottle (<https://www.mcmaster.com/42305T47/>) for aqueous waste with “Aqueous [chemical name (methylene blue or PFOS)] Rinsates.” Keep it outside the fume hood and be very careful to avoid getting any chemicals on the exterior of this container.
6. Label a 0.5- or 1-gallon waste container (<https://www.mcmaster.com/42955T2/>, <https://www.mcmaster.com/42955T4/>) for solid waste with “[chemical name] Contaminated Solids.” Store in the fume hood.
7. Label a 1.5 L HDPE or polypropylene Nalgene-type bottle for mixing solutions (<https://www.mcmaster.com/4280T37/>). Note: McMaster also sells LDPE bottles, which may be what is in the Creare stockrooms—do not use these as they can contaminate PFOS, and instead purchase bottles of known material from McMaster directly.
8. Have secondary containment for transport between Creare and Centerra available (<https://www.mcmaster.com/40015T81/>).

4.1.2 Preparing Methylene Blue Stock Solution in a Fume Hood

1. Label a 30 mL HDPE or polypropylene vial (<https://www.mcmaster.com/7940T53/>) with “Methylene Blue Aqueous Solution, 15 mM.”
2. Fill 10 mL distilled or DI water into the solution mixing bottle labeled above. Place on a drip tray in the fume hood.
3. Pre-crease/bend a polystyrene plastic disposable weighing tray to make it easier to transfer material.
4. Use a metal or plastic disposable lab spatula to weigh out the appropriate quantity of powdered material.
 - a. Methylene blue: 48.0 mg.


IM-22-04-080
April 14, 2022

5. Add the powdered material to the 10 mL of water and let dissolve. Can use a clean spatula to stir (either disposable, or use wet Kimwipes to clean and then rise, collecting Kimwipes and rinsate as hazardous waste).
6. Cap the bottle.

4.1.3 Preparing Diluted Methylene Blue Solutions in a Fume Hood

1. Fill 1 L distilled or DI water into the solution mixing bottle labeled above. Place on a drip tray in the fume hood.
2. Use a micropipette to measure 1 mL of 15 mM stock methylene blue solution prepared above into the 1 L of water.
3. Cap the bottle.

4.1.4 Preparing Diluted PFAS Solutions in a Fume Hood

1. Fill 1 L distilled or DI water into the solution mixing bottle labeled above. Place on a drip tray in the fume hood.
2. Pre-crease/bend a polystyrene plastic disposable weighing tray to make it easier to transfer material.
3. Use a metal or plastic disposable lab spatula to weigh out the appropriate quantity of powdered material.
 - a. PFOS: 0.54 mg.
 - b. PFOA: 0.50 mg.
 - c. PFHxS: 0.55 mg.
4. Add the powdered material to the 1 L of water and let dissolve. Can use a clean spatula to stir (either disposable, or use wet Kimwipes to clean and then rise, collecting Kimwipes and rinsate as hazardous waste). **Note:** Avoid fluorocarbon materials on the spatula; stainless steel or polypropylene are good choices.
5. Cap the bottle.

4.2 PROCEDURES FOR SETUP AND FILLING THE SYSTEM

Test all procedures with water before using hazardous materials. Only qualified system operators who have signed this safety IM and had Creare Chem Lab safety training and hazardous waste training may perform these procedures.

4.2.1 Work Area and Containment Materials

1. All chemical work must be performed in a fume hood. Wear 4 mil nitrile gloves when handling diluted solutions. Wear safety goggles or safety glasses and a face shield and a splash apron.
2. Have adequate spill pillows, paper towels, and Kimwipes available to be able to clean up a 1 L liquid spill.


IM-22-04-080
April 14, 2022

3. Verify that the fume hood blower is on and flow velocity is in the range of 60 to 100 ft/minute.
4. Label a five-gallon (19 L) polyethylene UN-compliant shipping jug (<https://www.mcmaster.com/4135T23/>) for aqueous waste with “Used Aqueous [chemical name (methylene blue or PFOS)] and Rinsates.” Keep it outside the fume hood and be very careful to avoid getting any chemicals on the exterior of this container.
5. Label a 0.5- or 1-gallon waste container (<https://www.mcmaster.com/42955T2/>, <https://www.mcmaster.com/42955T4/>) for solid waste with “[chemical name] Contaminated Solids.” Store in the fume hood.
6. Have a five-gallon polyethylene UN-compliant shipping pail with lid (<https://www.mcmaster.com/3995T439/>, <https://www.mcmaster.com/3995T459/>) for disposal of solid waste on hand and store it at the PFAS CAV bench in the main Centerra labs.
7. Label a 1.5 L HDPE or polypropylene bottle for temporary used material collection.
8. Ensure trays to collect material drained from the system are available:
 - a. Pump drain: 22-gauge stainless steel pan, 10" long, 6.5" wide, 2" high (<https://www.mcmaster.com/4191T1/>) or disposable polystyrene weighing dish, 330 mL capacity, 5.5" long (<https://www.mcmaster.com/17735T96/>).
 - b. Under heat exchanger and degasser: 22-gauge stainless steel pan, 12.75" long, 6.875" wide, 2.5" high (<https://www.mcmaster.com/4191T16/>).

4.2.2 Setup

1. Start chiller, set to 17°C. The target water is 22°C. Monitor water temperature using LabVIEW throughout experiment and adjust chiller set temperature as needed to achieve the target temperature (within +/- 1°C).
2. Make sure that the chiller is flowing through the heat exchanger and that the chiller bypass is closed.
3. Vent the pressure accumulator to 1 atm.
4. Ensure vacuum pump is vented into the fume hood. The vacuum pump is an oil-free diaphragm pump.
5. Ensure inlet reservoir and fluid lines are empty. Ensure all valves are closed.
6. Leak check the system:
 - a. Open the vent on the vacuum pump (if not already open).
 - b. Turn on vacuum pump switch.
 - c. Close the vacuum pump vent so that the pump is pulling vacuum only on the test loop and not on atmosphere.
 - d. Close V1 and V7. Close and cap N2.


IM-22-04-080
April 14, 2022

- e. Open V2, V3, V4, V5, V6, N1, and N2.
- f. Evacuate until $P3 < 25$ inHg.
- g. Close V5.
- h. Open the vacuum pump vent. Note: failure to do so may damage the pump or make it difficult to restart.
- i. Turn off vacuum pump switch.
WARNING: Do not shut off the vacuum pump with the vent closed!
- j. Wait five minutes and ensure $P3$ increases by < 1 inHg.

2. Start LabVIEW recording.

4.2.3 Fill

1. Ensure inlet tank and system are empty.
2. Close V1, V7, and N2.
3. Cap N2.
4. Open V2, V3, V4, V5, V6, and N1.
5. Fill inlet tank reservoir with 1 L fluid. (Inlet tank should be at atmospheric pressure.)
6. Close and latch the top of the reservoir.
7. Open the reservoir vent.
8. Turn on the vacuum pump (see Section 4.2.2, item 4, for how to correctly run the vacuum pump—pay attention to the vacuum pump vent to avoid damaging the pump).
9. Run vacuum pump until $P3 \leq 25$ inHg vac.
10. Shut V4 and V5 and turn off vacuum pump. Leave V6 open so that $P3$ reflects the pressure on the shell (gas) side of the degasser.
11. Crack and close V1 a few times. The goal is to fill the tubing between the inlet reservoir and V1.
12. Close V1.
13. Open V5 and V4 and turn on the vacuum pump until $P3 \leq 25$ inHg vac to remove air that entered the system when opening V1 to fill the line between the inlet reservoir and V1 with liquid.
14. Shut V5 and V4 and turn off vacuum pump. Leave V6 open.
15. Open V1 to fill the system. Wait three minutes to let it fill.

4.2.4 Degas Round 1

1. System pressure = 1 atm.
2. Close N1 and V3.


IM-22-04-080
April 14, 2022

3. Turn on the Liquiflo pump, running at 2 Hz (plug it in first).
4. Verify that V6 is open.
5. Open V3.
6. Open N1 fully.
7. Maintain these conditions for at least two minutes, observing any bubbles in the sight glass and flow meter. It is okay to tap the piping to release bubbles.
8. During these two minutes, close V6 temporarily and (barely) burp V4 to verify that there is water up to the V4 valve.
9. Reopen V6 and continue degassing.
10. Maintain approximately 25 inHg vac at P3 during the degassing process. (Turn on the vacuum pump and open V5 as needed. Close V6 when opening V5 to avoid sucking water back into the degasser.)
11. Turn off the vacuum pump and close V5.
12. Stop Liquiflo pump.
13. Close V1.
14. Close N1.
15. Close V3.

WARNING: Monitor the pressure when flowing fluid through the degasser. Do not leave N1 open and V3 closed and allow P1 to exceed 80 psia, as this may exceed the pressure rating of the degasser.

4.2.5 Degas Round 2

1. Add pressure to the accumulator to $P2 = 30 \pm 2$ psia. Verify that the system pressure responds to the accumulator pressure; if it does not, return to Degas Round 1, as there may still be a significant amount of gas in the system.
2. Use Figure 3 to determine the maximum pump speed for which the cavitation number remains above 1 at $P2 = 30$ psia for the installed orifice plate.
3. Turn on the Liquiflo pump and set to 2 Hz.
4. Verify that V6 is open.
5. Open V3.
6. Open N1 fully.
7. Once no bubbles are visible in the sight glass, increase Liquiflo pump speed to 4 Hz.
8. Once no bubbles are visible, increase Liquiflo pump speed in increments of 2 Hz up to the maximum pump speed found in step 2. Monitor P1 while increasing the pump speed and do not allow it to exceed 80 psia (stop increasing pump speed before the value found in step 2 if needed).


IM-22-04-080
April 14, 2022

9. Maintain for at least two minutes, until no bubbles are visible through the sight glass or in the flow meter.
10. If stuck bubbles are still visible in the flow meter after two minutes at the maximum pump speed at $P2 = 30$ psia, conduct a third round of degassing at $P2 = 60 \pm 2$ psia. Use Figure 3 to determine the maximum pump speed for which the cavitation number remains above 1 at 60 psia for the installed orifice plate. Then repeat steps 3 to 9.
11. Close N1, then V3.

WARNING: Do not leave N1 open and V3 closed and allow P1 to exceed 80 psia, as it may exceed the pressure rating of the degasser.

4.3 PROCEDURES FOR RUNNING THE SYSTEM AND TAKING SAMPLES

4.3.1 Collect Pretreatment Sample

1. Turn off the Liquiflo pump. Relieve the pressure on the accumulator (it may be a little below 1 atm).
2. Open V1. P2 will bounce back to 1 atm.
3. Close V2.
4. Place a drip tray under the N2 outlet.
5. Uncap N2.
6. Open N2.
7. Collect the first 5 mL and discard as hazardous waste.
8. Collect the next 2 mL in the sample container for analysis.
9. Close N2.
10. Close V1.
11. Wipe threads at N2 outlet and recap N2. Discard wipe as hazardous waste.

4.3.2 Run System

1. Increase Liquiflo pump speed to desired pump speed.
2. Start timer (or note elapsed time (EL) on LabVIEW).
3. Top off pressure in the accumulator until P2 equals desired value (30 to 90 psia ± 1 psia)
4. Run for desired experiment time, initially estimated at 60 minutes. An operator who has read and signed this safety IM must be present and monitoring the system at all times.

4.3.3 Post-Treatment Sample

Follow same method as pre-treatment sample above.


IM-22-04-080
April 14, 2022

4.4 PROCEDURES FOR EMPTYING THE SYSTEM

4.4.1 Required Number of Rinses

To fully empty the system and consider it sufficiently clean, change the operating fluid, or remove it from the fume hood for additional cleaning, transport, or storage, the residual level of PFAS contaminants must be below New Hampshire guidelines for drinking water of 15 ppt for PFOS, 12 ppt for PFOA, and 18 ppt for PFHxS. The table below gives the required number of rinses for a given residual volume that is not removed when draining the system, calculated according to:

$$C(x) = C_0(r/V)^x$$

where C is the concentration after rinse number x , C_0 is the initial concentration of 500 ppb, V is the total system volume of 1000 mL, and r is the residual volume not removed when draining the system and expected to be around 50 to 100 mL. If only 930 mL out of a starting 1000 mL can be removed when draining the system, four rinses are expected to be required for each of the PFAS chemicals.

# Rinses	Residual Volume (1000 mL total volume)		
	PFOS (15 ppt)	PFOA (12 ppt)	PFHxS (18 ppt)
3	< 31 mL	< 28 mL	< 33 mL
4	< 74 mL	< 70 mL	< 77 mL
5	< 124 mL	< 119 mL	< 129 mL

The requirements for methylene blue are not as stringent, as this material is not considered hazardous waste, though it should not be disposed down the drain. Three rinses are sufficient for clearing methylene blue from the system. Fewer rinses may be necessary between experiments with the same chemical, and the number required is left to the discretion of the project team.

4.4.2 System Volume

The amount of fluid removed from the system at each step is shown in the table below. Steps 1 through 3 can be done without any disassembly. Steps 4 through 7 require disassembly. Values are based on starting with 1000 mL in the system. More details about each step are below. The expected volumes of each component (if completely full of water) are as follows:

- HX: 150 mL
- Degasser: 85 mL
- Pump (residual water): 65 mL


IM-22-04-080
April 14, 2022

Step #	Step	Fluid Removed (mL)	Total Fluid Removed (mL)
1	Open V1 to empty from inlet reservoir, no air pressure applied	620	620
2	Apply pressure at V5 with shop air	70	690
3	Open pump port	95	785
4	Empty degasser	70	855
5	Empty HX	30	885
6	Empty flow meter and spectrometer sight glass	25	910
7	Apply pressure where the HX was, collect water from pump port	20	930/1000 (final value)

4.4.3 Setup Emptying Process

1. Turn off chiller.
2. Relieve any remaining pressure on the accumulator (P2 should equal 1 atm).
3. Verify that the pump is off.
4. Save LabVIEW data (if done with data-collection).
5. Close V1.
6. Keep closed: V4, V5, V6, and N2.

4.4.4 Empty Water Trap Into Inlet Reservoir

1. Disconnect the tube from the top of the Tee between V6 and V4 (the line that goes to the water trap). This releases the vacuum in that line.
2. Put the end of this tube in the inlet reservoir port.
3. Unlock the inlet reservoir cap to vent to atmosphere.
4. Disconnect the vacuum pump line to V5 at the vacuum pump and attach a regulated pressure source. Set the maximum pressure to 1 psig.
5. Open V5 and apply 1 psig pressure. This will push the water in the trap to the inlet reservoir.
6. Close V5.

4.4.5 Empty Inlet Reservoir

1. Open V1.
2. Open N1, V3, and V2.


IM-22-04-080
April 14, 2022

3. Take off N2 cap, connect tubing in place of the cap.
4. Put end of tubing in collection reservoir (labeled above, <https://www.mcmaster.com/4280T37/>).
5. Open N2. This should start the system draining beginning at the inlet reservoir.
6. Open V5 and apply pressure, keeping P3 below 3 psi. Continue applying pressure until no more fluid is flowing into the collection reservoir. May need to pulse the pressure to push out slugs of fluid.
7. Close V5.
8. Close V2.

4.4.6 Empty from Pump Port

1. Put shallow collection reservoir (<https://www.mcmaster.com/17735T96/> or <https://www.mcmaster.com/4191T1/>) below fill port.
2. Open V7 and drain right from the valve output since the flow is so slow.
3. Open V5 to apply pressure. Expect the fluid flow to be very slow.
4. Close V5.
5. Keep V7 open while emptying other parts of the system to allow it to slowly drain.

4.4.7 Empty Degasser

1. Close N1 and V3.
2. Put tray below to catch drips and spills (<https://www.mcmaster.com/4191T16/>).
3. Disconnect the fitting on the degasser side of V3 and tip that line to face upward.
4. Disconnect the fitting on the degasser side of N1. Note: fluid spilled when we detached the second end, so make sure to have a catch below.
5. Apply pressure to one end of the degasser (not a regulated source). It may be possible to keep one end connected to the system during this step to reduce the possibility of spillage. Use Kimwipes to wipe drips from the ends of the degasser, and discard wipes as hazardous waste.
6. Reattach both ends of the degasser to the system.

4.4.8 Empty Heat Exchanger (HX)

1. Put a tray below HX to catch drips or spills (<https://www.mcmaster.com/4191T16/>).
2. Disconnect both ends of the HX.
3. Tip the HX back and forth to release any water in the HX. Be careful to contain drips to the drip tray and avoid sprayed droplets.



IM-22-04-080
April 14, 2022

4.4.9 Empty Flow Meter (FM) and Spectrometer Sight Glass

1. Put a tray below to catch drips or spills (<https://www.mcmaster.com/4191T16/>).
2. Remove the spectrometer from the sight glass.
3. Disconnect flow meter connect to the return tubing to the pump (the other end was connected to the HX).
4. Tip the FM and sight glass back and forth to release any water in the tubing or either component. Be careful to contain drips to the drip tray and avoid sprayed droplets.

4.4.10 Return to Emptying Pump and Fluid Lines

1. Cap one of the open tube ends where the HX, sight glass, and FM were previously connected.
2. Apply pressure to the other port. Use low pressure and verify that this does not generate sprayed droplets.
3. Swap cap and pressurized side and repeat.
4. When finished, reattach the HX, sight glass, and FM.

4.4.11 Finish Emptying System

1. Empty the collection reservoirs from under the pump drain port and HX into the temporary waste collection bottle. Use a funnel as needed.
2. Squirt-rinse the collection reservoirs and empty into temporary waste collection bottle.
3. Empty the temporary waste collection bottle into the hazardous waste container, **being very careful not to spill any hazardous material on the outside of the container.** Use a funnel to avoid drips on the outside of the hazardous waste container.
4. At this point, some water will still be visible in the sight glass. Expect that there is more water in the tubing and still some water in the degasser. We estimate about 70 mL out of the original 1000 mL will still be in the system.
5. Reassemble the system, fill it with clean water (following Sections 4.2.1 through 4.2.4) and then re-empty it the desired number of times according to Section 4.4.1, collecting the rinsates as hazardous waste each time. Use the solution rinsing bottle to fill the system so that it is also rinsed out.
6. When done flushing the system, soak up any remaining fluid in the inlet reservoir using wipes. Dispose of these as hazardous waste.
7. Dry the sample port between N2 and the end cap with a cotton swab.



IM-22-04-080
April 14, 2022

4.5 PROCEDURES FOR CLEANUP AND DISPOSAL OF MATERIALS

1. Make sure all liquid-exposed tools, catch trays, funnels, and catch containers have been thoroughly squirt-rinsed with DI at least four times. Collect the rinsate in the waste container. If these items will be used again in the near future, they may be isolated and labeled as a contaminated item in the hood until used again. If they will not be used again in the near future, they should receive a final washing with Joy dishwashing liquid, water, and then DI in the laboratory sink (but only after the thorough squirt-rinsing noted above). Items that have been cleaned following these procedures may be returned to general use, but should be labelled "Potentially Contaminated With PFAS."
2. Pour all liquid waste into the labeled five-gallon liquid hazardous waste jug. Be very careful to avoid getting any liquid on the outside of this container.
3. Seal the liquid waste jug, and double bag in trash bags, tying each off. Ensure the label is still readable, or add an additional label outside the bag.
4. Store in secondary containment under the PFAS CAV bench in the main labs Centerra.
5. Close solid waste jars and place all solid waste jars as well as other solid waste (such as contaminated containers used to mix solutions or temporarily hold waste) into the solid waste can. Seal the lid onto the can. Avoid contaminating the exterior of the can.
6. Double bag the solid waste can, tying each off, and ensure a label is visible from the outside. Store under the PFAS CAV bench in the main labs at Centerra.
7. Contact RPK to arrange hazardous waste pickup when a container is full or at the conclusion of testing.


IM-22-04-080
April 14, 2022

5 SAFETY REVIEW APPROVAL

Safety Procedures Read and Understood:

I have read and understand the hazards and safety precautions described above and in the referenced documents, and I agree to follow the safety measures described.

Project Engineer:	(RGilmore)	<u>Rachel H Gilmore</u> <small>Rachel H Gilmore (Apr 15, 2022 10:42 EDT)</small>	Date: <u>Apr 15, 2022</u>
Project Engineer:	(MGIzenson)	<u>Michael Izenson</u>	Date: <u>Apr 15, 2022</u>
Project Engineer:	(CLD)	<u>Clayton Deery</u>	Date: <u>Apr 15, 2022</u>
Project Engineer:	(DKromer)	<u>Daniel Kromer</u> <small>Daniel Kromer (Apr 15, 2022 14:01 EDT)</small>	Date: <u>Apr 15, 2022</u>
Technician:	(ADuffy)	<u>Alan Duffy</u> <small>Alan Duffy (Apr 18, 2022 09:41 EDT)</small>	Date: <u>Apr 18, 2022</u>
Technician:	(KTM)	<u>Nick M...</u>	Date: <u>Apr 18, 2022</u>
Spill Team:	(RPK)	<u>Ray Kendall</u> <small>Ray Kendall (Apr 18, 2022 09:51 EDT)</small>	Date: <u>Apr 18, 2022</u>
Spill Team:	(JWO)	<u>John W. Osborne</u>	Date: <u>Apr 18, 2022</u>

Safety Review Approval to Proceed:

Safety Officer:	(MXS)	<u>Michael Swanwick</u> <small>Michael Swanwick (Apr 19, 2022 08:24 EDT)</small>	Date: <u>Apr 19, 2022</u>
-----------------	-------	---	---------------------------

1010427.01.001/btt